Carbon isotopes and systematics of Icelandic low-temperature geothermal waters

Ríkey Kjartansdóttir

Faculty of Earth Sciences
University of Iceland
2014

Carbon isotopes and systematics of Icelandic low-temperature geothermal waters

Ríkey Kjartansdóttir

60 ECTS thesis submitted in partial fulfillment of a
Magister Scientiarum degree in Geology

Advisor
Andri Stefánsson

Faculty Representative
Ingvi Gunnarsson

Faculty of Earth Sciences
School of Engineering and Natural Sciences
University of Iceland
Reykjavík, October 2014

Carbon isotopes and systematics of Icelandic low-temperature geothermal waters
C isotopes & systematics of Icelandic low-T geothermal waters
60 ECTS thesis submitted in partial fulfillment of a *Magister Scientiarum* degree in Geology

Faculty of Earth Sciences
School of Engineering and Natural Sciences
University of Iceland
Sturlugata 7
101, Reykjavik
Iceland

Telephone: 525 4000

Bibliographic information:
Ríkey Kjartansdóttir, 2014, *Carbon isotopes and systematics of Icelandic low-temperature geothermal waters*, Master's thesis, Faculty of Earth Sciences, University of Iceland, pp. 39.

ISBN XX

Printing: Háskólaprent
Reykjavík, Iceland, October 2014

Abstract

The carbon chemistry and stable carbon isotope systematics of low-temperature geothermal waters in Iceland was studied. The waters had temperatures ranging from 3 to 97°C, pH between 6.18 and 10.15 as well as dissolved inorganic carbon concentration from 1.8 to 2853 ppm. The carbon isotopes were found to be in the range $\delta^{13}C$ -1.46 to -13.96‰. The geochemistry of CO_2 and its sources and reactions in low-temperature geothermal water was approached in three ways; by carbonate mineral saturation, a component mixing model and by reaction path isotope modelling. Low-temperature geothermal waters were observed to be calcite saturated, suggesting that calcite may possibly form in low-temperature ground water systems. The source of the carbon in the water and the possible formation of calcite, along with the stable carbon isotope systematics cannot be explained simply by rock dissolution, atmospheric CO_2 input and organic matter decay. Instead, progressive basalt dissolution, aqueous speciation, and calcite formation play a major role in carbon isotope systematics and the carbon concentration of the low-temperature geothermal water. For waters that contain low CO_2 concentrations (<50 ppm) and low $\delta^{13}C$ values (-5 to -15‰) the CO_2 is thought to be derived from both atmospheric sources and primary rock dissolution. This is due to the variations of CO_2 concentrations and $\delta^{13}C$ values generated by the concentration of CO_2 and the exact $\delta^{13}C$ content of the basalt, and due to carbon isotope fractionation upon water-rock interaction. However, waters that contain high CO_2 concentrations and high $\delta^{13}C$ values cannot be explained without the introduction of a highly concentrated CO_2 source with a $\delta^{13}C$ value of less than -3‰. This source cannot be carbonate dissolution at shallow depth within the crust, as this would result in too low CO_2 concentrations. Mantle degassing through the crust is also unlikely as this would result in too low $\delta^{13}C$ values. Presently, an alternative CO_2 source of unknown origin has therefore been introduced as the cause of elevated CO_2 low-temperature geothermal waters in Iceland.

Útdráttur

Efnafræði kolefnis og virkni kolefnis samsæta í lághita jarðhitavatni á Íslandi var rannsakaður. Vatnið var á hitabilinu 3° - 97°C, pH vatnsins var 6.18-10.15 og magn uppleysts ólífræns kolefnis var á bilinu 1.8-2853 ppm. Kolefnis samsæturnar $\delta^{13}C$ voru á bilinu -1.46 til -13.96‰. Jarðefnafræði CO_2, uppruni og efnahvörf í lághita jarðhitakerfum var rannsakaður á þrjá vegu, með mettun kolefnis steinda, blöndunar líkani og með jarðefnafræðilegum samsætulíkanreikningum. Lághita jarðhita vatnið var kalsít mettað, sem bendir til þess að kalsít geti mögulega myndast í lághita grunnvatnskerfum. Uppruni kolefnis í vatninu og myndun kalsítsins ásamt virkni stöðugu samsætanna er ekki hægt að útskýra með uppleysingu á bergi, CO_2 frá andrúmsloftinu eða með niðurbroti lífræns efnis. Í staðinn spila stigvaxandi uppleysing basalts, efnasambönd í vatnslausn og myndun kalsíts stórann þátt í virkni kolefnis samsæta og styrk kolefnis í lághita jarðhita vatni. Uppruni CO_2 í vatni með lágan styrk CO_2 < 50ppm og lág $\delta^{13}C$ gildi (-5 til -15‰) er talinn vera bæði uppleysing á frumbergi og andrúmsloftið, breytileiki í styrk CO_2 og $\delta^{13}C$ er talinn stafa styrk CO_2 og gildi $\delta^{13}C$ í berginu sjálfu. Aftur á móti er ekki hægt að útskýra vatn með háan CO_2 styrk og há $\delta^{13}C$ gildi, án þess að kynna til sögunnar upptök með háan styrk CO_2 og $\delta^{13}C$ gildi lægri en -3‰. Þessi uppruni getur ekki verið vegna uppleysingar á karbónati á litlu dýpi í jarðskorpunni, þar sem það myndi leiða til hárra $\delta^{13}C$ gilda og lágs CO_2 styrks. Afgösunum möttulsins í gegnum jarðskorpuna er einnig ólíklegur þar sem það myndi líklega leiða til of lágra $\delta^{13}C$ gilda. Önnur CO_2 uppspretta af ókunnum uppruna hefur þ.a.l. verið kynnt sem orsakavaldur hækkaðs CO_2 styrks í lághita jarðhitavatni á Íslandi.

Table of Contents

List of Figures ..... **x**

List of Tables ..... **xii**

Acknowledgements ..... **xiii**

1 Introduction **1**

2 Low-temperature geothermal systems in Iceland and sample location **3**
2.1 Southern Lowlands 4
2.2 West Coast 5
2.3 Skagafjörður 5

3 Sampling and analysis **7**
3.1 Major element sampling and analysis 7
3.2 Carbon-isotope sampling and $\delta^{13}C$ determination 7

4 Geochemical modelling **9**
4.1 Aqueous speciation and mineral saturation 9
4.2 Isotope mixing model of Sveinbjörnsdóttir et al. (1995) 9
4.3 Reaction path modelling 10
4.4 Reaction path isotope modelling 12
4.5 Carbon isotope fractionation factors 15

5 Water chemistry and carbon isotope systematics **19**

6 Geochemistry of CO_2 and the source and reactions of carbon in low-temperature geothermal systems **23**
6.1 Aqueous speciation of dissolved inorganic carbon 23
6.2 CO_2 source in groundwaters and the mixing model proposed by Sveinbjörnsdóttir et al. (1995) 25
6.3 CO_2 source in groundwaters and reaction path modelling 27

7 Conclusions **35**

References **37**

List of Figures

Figure 1 The location of sample sites. 4

Figure 2 The CO_2 extraction line at the University of Iceland. 8

Figure 3 Isotope fractionation factors as a function of 1/T in Kelvin. Shown are various experimentally derived values together with the fit obtained in this study. 17

Figure 4 The relationship between pH and temperature, and CO_2 and Cl in the sampled waters. 20

Figure 5 The relationship between $\delta^{13}C$ and temperature, pH, CO_2, and Cl. 21

Figure 6 The relationship between $\delta^{13}C$ and CO_2 for sampled fluids in Iceland and rocks together with some reference samples. 21

Figure 7 Aqueous speciation distribution of CO_2 containing aqueous species in the water samples. 24

Figure 8 Mineral saturation states with respect to common carbonate minerals. 25

Figure 9 The results of the reaction path simulations for basalt dissolution into meteroic water initially saturated with atmospheric CO_2. Shown are the aqeuous carbon species distribution, pH, and secondary mineral formation as a function of reaction progress (ξ). 28

Figure 10 The results of the reaction path simulations for basalt dissolution into meteroic water initially containing 5000 ppm CO_2. Shown are the aqeuous carbon species distribution, pH, and secondary mineral formation as a function of reaction progress (ξ). 29

Figure 11 The results of the reaction path simulations for basalt dissolution into meteroic water initially saturated with atmospheric CO_2. The $\delta^{13}C$ value of the meteroic water and basalt was taken to be $\delta^{13}C$ -7‰. Shown are the aqeuous carbon species distribution, pH and secondary mineral formation as a function of reaction progress (ξ). 31

Figure 12 The results of the reaction path simulations for basalt dissolution into meteroic water initially containing 5000 ppm CO_2. The $\delta^{13}C$ value of the meteroic water was $\delta^{13}C$ -3‰ and basalt was taken to be $\delta^{13}C$ -7‰. Shown are the aqeuous carbon species distribution, pH, and secondary mineral formation as a function of reaction progress (ξ) and pH. 32

Figure 13 The comparison between the measured and simulated $\delta^{13}C$ and pH and $\delta^{13}C$ and CO_2 relationships. The blue and red curves represent the

modelled trends for waters initally being CO_2 saturated and having 5000 ppm CO_2, respectively. The shaded areas show the simulated $\delta^{13}C$ and CO_2 relationship. 33

List of Tables

Table 1 Chemical composition of Stapafell glass used in model calculations. 11

Table 2 Starting water composition used in the reaction path modelling. 11

Table 3 Minerals included in the reaction path and reaction path isotope simulations. 12

Table 4 The initial conditions of the reaction path and reaction path isotope simulations 15

Table 5 Carbon isotope fractionation factors derived in this study. 18

Table 6 Chemical analysis of geothermal waters 22

Table 7 The source of CO_2 in the water samples according to the model proposed by Sveinbjörnsdóttir et al. (1995). 26

.

Acknowledgements

Firstly, I would like to thank my supervisor, Andri Stefánsson for allowing me to work on this project and to encourage me to work independently. It has been a great learning experience. Árný Erla Sveinbjörnsdóttir and Rósa Ólafsdóttir I would like to thank for their assistance with the CO_2 extraction line and general interest in the thesis progress.

Nicole Keller gets my best thanks for assistance in the lab, for measuring the ICP-OES samples and always being willing to help. Field assistance was much appreciated from my fellow students Ragnheiður Ásgeirsdóttir and Jóhann Gunnarsson Robin, along with a great deal of help from my boyfriend Helgi Guðjónsson who has tagged along on numerous sampling trips and given moral support during these past 2 years.

Lastly, I would like to thank all my friends and fellow students in Askja especially Halldóra Björk Bergþórsdóttir, Ragnheiður Ásgeirsdóttir and Jón Bjarni Friðriksson, for always being willing to talk and listen to me during these past 2 years. My fellow geochemist in the Geysir group I thank for lively discussions and support. This thesis was funded by the Landsvirkjun Research Fund (Orkurannsóknasjóður Landsvirkjunar), a funding which was much appreciated.

1 Introduction

Low-temperature geothermal areas in Iceland have been widely used for district heating, heating of swimming pools and other industrial uses such as heating of greenhouses and fish farming (e.g. Arnórsson, 1995a; Axelsson et al., 2010). Due to their availability and usefulness in district heating, low-temperature areas have been investigated quite extensively over the past few decades, both in terms of heat source and chemistry (see Arnórsson, 1995a).

Carbon is the 15th most common element in the Earth's crust. Dissolved inorganic carbon (DIC) is among the major elements in low- and high-temperature geothermal fluids, and is found both within the liquid and vapor phase (Arnórsson, 1995a,b). Three different carbon isotopes exist in some abundance: carbon 12, 13 and 14. Other carbon isotopes are known but they have extremely short half-life (Sharp, 2007). Generally ^{12}C is the most abundant isotope in the Earth's system accounting for 98.89% of all carbon followed by ^{13}C consisting of 1.11% of all carbon (Hoefs, 1997). ^{12}C and ^{13}C are the two stable isotopes of carbon. The ^{14}C isotope is radioactive with a half-life of ~5730 years. ^{14}C is extensively used for radiocarbon dating.

The main carbon reservoirs in the crust are in the form of inorganic carbon that is found in sedimentary rocks, organic carbon and carbon in crystalline rocks (Sharp, 2007).The biggest organic reservoirs are sedimentary rocks, soil, fossil fuels, and plants (Gíslason, 2012). Inorganic carbon forms chemical bonds with Ca and O forming $CaCO_3$, better known as calcite or aragonite depending on the crystal structure of the formed mineral (Gíslason, 2012). Calcite is a common alteration mineral in geothermal systems (Browne, 1978; Sveinbjörnsdóttir et al., 1995). Calcite precipitates easily from the water when calcite saturation has been reached, but its solubility in water increases with increased CO_2 pressure and decreasing temperatures. Other known carbonates include, magnesite, siderite, dolomite, ankerite, dawsonite and various types of solid solutions (Deer et al., 1994).

Isotopes can be used as tracers. The ratio between ^{12}C and ^{13}C known as $\delta^{13}C$ is useful in tracing the origin of carbon in waters, since materials have variable values of $\delta^{13}C$. Compared to organic matter, Earth's atmosphere is enriched in ^{13}C, giving the atmosphere a $\delta^{13}C$ value of -8 ‰. In recent years the $\delta^{13}C$ value of the atmosphere has been steadily decreasing, going from -6 to -8 (Sharp, 2007). Physical processes in plants during photosynthesis favor ^{12}C over ^{13}C during the process resulting in lower $\delta^{13}C$ value in plants. Difference in photosynthesis cycles also influence the $\delta^{13}C$ value of the plants, categorizing them into C_3 and C_4 plants (Marshall et al., 2007). C_3 plants are more common in high latitude areas including Iceland. C_3 plants are isotopically lighter than C_4 with $\delta^{13}C$ values in the range of -23 to -33‰ (Sharp, 2007). Calcite in basaltic rocks has a $\delta^{13}C$ of -4 ‰ (Sveinbjörnsdóttir et al., 1995) whereas the typical mantle value is -5 to -6 ‰ (Sharp, 2007). Recent studies of $\delta^{13}C$ in basaltic glass in Iceland, give a large range of values for basaltic rock from -3.6 to -27.1‰. These values indicate carbon fractionation upon magma degassing (Barry et al., 2014).

Previous research on the origin of carbon in low-temperature areas in Iceland is rather limited. Sveinbjörnsdóttir et al. (1995) created a conceptual model on the origin of carbon in Icelandic groundwaters. The model was mostly meant to shed light on the origin of ^{14}C and to determine the age of groundwaters but measurements and calculations were

also carried out for $\delta^{13}C$. There the origin of carbon was thought to be three-fold: organic, atmospheric, and rock leached. Arnórsson and Barnes (1983) used $\delta^{13}C$ to trace the origin of carbon in CO_2 rich springs on the Snæfellsnes peninsula, without really coming to a definite conclusion, except for the fact that the carbon could not be leached from the surrounding rocks. No research was published on $\delta^{13}C$ in Icelandic waters or rocks for almost 20 years, until a research by Barry et al. (2014) came out. There, fresh glass samples from basaltic rocks, along with geothermal water and fumarole samples were collected to estimated and constrain the CO_2 fluxes associated with Mid-Atlantic ridges. No clear picture was drawn up regarding the origin of $\delta^{13}C$ in geothermal water. However they conclude that basaltic glass is heavily degassed in regard to CO_2 and $\delta^{13}C$ values are probably quite biased due to carbon fractionation during cooling and possible organic contamination of the samples. Despite these researches, the origin of carbon in low-temperature geothermal fluid and natural waters still remains unclear.

The purpose of this thesis is to try to trace the origin of carbon in low-temperature geothermal waters in Iceland using $\delta^{13}C$ systematics and CO_2 geochemistry. Samples were collected of low-temperature waters ranging in temperatures from 3°C to 97°C and with a pH range of 6.18-10.15. In order to explain the source and reactions of CO_2 in the waters, component mixing model was applied (e.g. Sveinbjörnsdóttir et al., 1995) as well as gas-water-rock geochemical model whereas an attempt was made to simulate the geochemical reactions of importance and the associated carbon isotope fractionations.

2 Low-temperature geothermal systems in Iceland and sample location

Geothermal activity in Iceland has been categorized into two separate groups, based on their origin and temperature, in low- and high-temperature geothermal systems (Böðvarsson, 1961). High temperature geothermal systems are defined as systems within the active volcanic belts with temperatures of over 200°C at 1000 m depth whereas low-temperature geothermal activity has been characterized by temperature ranging from ambient (6°C) to 150°C at 1000 m depth. Low-temperature geothermal activity is widespread in the Quaternary and Tertiary formations west of the active rift zones, in the West and North of Iceland as well as on the Southern Lowlands (Arnórsson, 1995a; Axelson et al., 2010). The low-temperature geothermal activity is thought to be heavily related to the stress conditions of the crust, and also to the formation of fractures and faults (Björnsson et al., 1990).

Waters in low-temperature areas are usually alkaline due to water-rock interaction (Arnórsson, 1995a; Arnórsson and Andrésdóttir, 1995). The waters are typically low in dissolved solids (<500 ppm). Major constituents include Si, Na, K, Ca, Mg, Al, Si, Cl, F, SO_4, H_2S and CO_2. The source of dissolved solids in low-temperature waters in Iceland is considered to be originated from the atmosphere, surrounding rocks and organic matter (Sveinbjörnsdóttir et al., 1995). The source water in the systems is either meteoric or from seawater or a mixture thereof, ranging in age from present to older than 10,000 years (Arnórsson and Andrésdóttir, 1995; Sveinbjörnsdóttir et al., 1995).

In this study, non-thermal and low-temperature geothermal waters were collected from various locations in the Southern-Lowlands, West and North of Iceland. Sample locations are shown in Figure 1 and a general overview of the sampled fields is given below.

Figure 1 The location of sample sites.

2.1 Southern Lowlands

The second largest low-temperature geothermal area in Iceland is located in the Southern Lowlands. It has an average discharge of 330 l/s and covers an area of about 700 km^2 (Arnórsson, 1970). Low-temperature geothermal activity in the Southern Lowlands is widespread where active seismicity takes place, especially on E-W trending faults. The seismicity zone is called the South Iceland Seismic Zone. This zone takes up transforms between the East and West Volcanic Zones (Einarsson, 1991). Chemical composition of geothermal waters in this area can vary with distance from sea, though especially the content of Cl in the water. After the last glaciation the sea transgressed into the Southern

Lowlands and percolated into the bedrock, resulting in higher Cl concentration in the geothermal waters on the flat-lying area (Arnórsson and Andrésdóttir, 1995).

A total of 13 samples were collected in the Southern Lowlands, 2 from cold springs, 1 river sample, and 10 geothermal samples. Of the geothermal samples 8 were from drill holes and 2 from thermal springs.

2.2 West Coast

West of the volcanic zone most of the geothermal activity is concentrated in the Borgarfjörður region, although it can also be found in the area around Breiðafjörður, including Snæfellsnes peninsula (Jóhannesson, 1982). Geothermal activity on Snæfellsnes peninsula is mostly confined to the northern part (Torfason, 2003), however cold CO_2 springs are quite common on both sides of the peninsula (Jóhannesson, 1982).

The Borgarfjörður geothermal area is the largest low-temperature geothermal area in Iceland, with a natural discharge of 450 l/s (Georgsson et al., 1980), and is located on the western side of the Western Volcanic zone (Arnórsson and Ólafsson, 1986). The area can be divided into 5 geothermal systems based on water chemistry. Of the 5 systems Reykholt is the most powerful one (Georgsson et al., 1980).

Numerous faults have been identified in the Borgarfjörður area. These faults are considered to have mostly a twofold origin: firstly NE-SW trending fault swarms that are caused by crustal dilation in the nearby rift zone, and secondly, faults that are formed due to stress fields with lateral shear forces. These faults are thought to belong to the Snæfellsnes Fracture zone which formed due to shifting in rift centers 6.5 M.y.a. (Jóhannesson, 1980).

The Snæfellsnes peninsula is heavily fractured; the fractures are a relic of the Snæfellsnes rift zone which was very active unit about 6.5 M.y.a. (Jóhannesson, 1980). Geothermal activity on the Snæfellsnes peninsula is very sparse, but many CO_2 springs have been located there. Thermal CO_2 springs can be found at Lýsuhóll, with the highest temperature measured at 57°C (Jóhannesson, 1982). The cold CO_2 springs can have variable flow rates and are very dependent on weather. Dry weather can result in lowering of the water table to such an extent that only CO_2 gas emerges at the spring basin (Arnórsson and Barnes, 1983).

Samples were collected from 5 different locations on the Western part of Iceland. These include geothermal well waters, thermal springs and CO_2 springs on the Snæfellsnes peninsula.

2.3 Skagafjörður

Geothermal heat in the Skagafjörður area is thought to be related to both volcanic activity and spreading at a segment of the Mid-Atlantic ridge, known as Kolbeinsey Ridge (Arnórsson and Gíslason, 1990). Low-temperature geothermal activity is widely distributed in the valleys of both Skagafjörður and Eyjafjörður, and is often seen to emerge at dyke contacts as well as through faults (Arnórsson, 1995a). Thermal springs in the Skagafjörður valley have temperatures ranging from ambient (6°C) to 90°C. Recharge to most of the springs below 60°C is driven by hydraulic head in the surrounding mountains (Arnórsson and Sveinbjörnsdóttir, 2000).

Samples in the Skagafjörður area are 4 in total, Sjávarborg, Hofsvellir, Varmilækur and Víðivellir. 3 of the sampling sites are in the western part of the valley, and 1 in the eastern part.

3 Sampling and analysis

3.1 Major element sampling and analysis

In this study 24 samples were collected from several low-temperature geothermal systems in Iceland during 2012 to 2013. The sample sources included drill hole discharges, as well as thermal and non-thermal springs.

The water samples were analyzed for major elements (pH, Si, B, Na, K, Ca, Mg, Fe, Al, F, Cl, SO_4, CO_2 and H_2S), as previously described in detail (Arnórsson et al., 2006). The samples for major ions both cations and anions were filtered through 0.2 µm filters (cellulose acetate) into HDPE bottles, acidified to 1% HNO_3 (Suprapur® Merck) and analyzed using ICP-OES. Samples for determination of total dissolved inorganic carbon (DIC) were cooled down if necessary using an in-line cooling coil, collected into amber glass bottles, and analyzed using modified alkalinity titration. The pH and H_2S were determined in untreated samples on site using pH electrodes and H_2S by precipitation titration.

In most cases the analytical precision based on duplication analyses was found to be <3% at the 95% confidence level.

3.2 Carbon-isotope sampling and $\delta^{13}C$ determination

Samples for determination of carbon-13 ($\delta^{13}C$) and for dissolved inorganic carbon (DIC) were collected into 1 liter amber glass bottles. Between 2-3 drops of $HgCl_2$ (3.7g/50mL) were added to the sample to prevent any photosynthesis upon sample storage. To prevent any air contamination, the sample water was pumped using a peristaltic pump. The outflowing silicon tube was put to the bottom the bottle, out of which water was then allowed to flow, after filling for some time, before being closed with an air-tight lid. For waters containing high-concentrations of CO_2, samples were collected into a flow through gas-bottle fitted with vacuum caps to prevent degassing upon sample storage. About 5 ml of sample was replaced by 5M NaOH through septa on the gas-bottle to raise the pH and prevent possible CO_2 loss.

The dissolved inorganic carbon from the sample bottles were extracted for purification and $\delta^{13}C$ determination, using a carbon isotope extraction line available at the University of Iceland. The samples were run in two batches. The first batch was run in May 2013, and the second one in November and December 2013. The CO_2 extractions were carried out as described in McNichol et al. (1994). First, the extraction line was evacuated and a certain amount of sample was allowed to flow into an evacuated glass bottle. An amount of 4 ml of 85% H_3PO_4 was added to the sample once it had entered the glass bottle, in order to lower the pH of the sample. N_2 was bubbled through the sample and the CO_2 was chased from the sample into cooling traps. All moisture was first cryogenically extracted using liquid N_2-alcohole mixture (-75° to -80°C). This was

followed by cryogenic CO_2 extraction using liquid N_2, and a cycle of re-thawed and cryogenic CO_2 extraction into a glass finger. The finger was then thawed and the pressure of CO_2 was read from a pressure transducer. The gas was then put into small glass ampules, 0.3 mgC for $\delta^{13}C$ analysis. The ampules were then closed using a gas burner. A setup of the extraction line is shown in Figure 2.

Analyses of $\delta^{13}C$ were carried out using an IsoPrime stable isotope ratio mass spectrometer at the Aarhus AMS Center, Denmark. The carbon isotope composition of a sample is given by (Coplan, 1994),

$$\delta^{13}C(‰) = \left(\frac{\left({}^{13}C/{}^{12}C\right)_{sample}}{\left({}^{13}C/{}^{12}C\right)_{VPDB}} - 1 \right) \cdot 1000$$

whereas VPDB is the reference sample Vienna Pee Dee Belemnite. The standard deviation of the measurement was 5%.

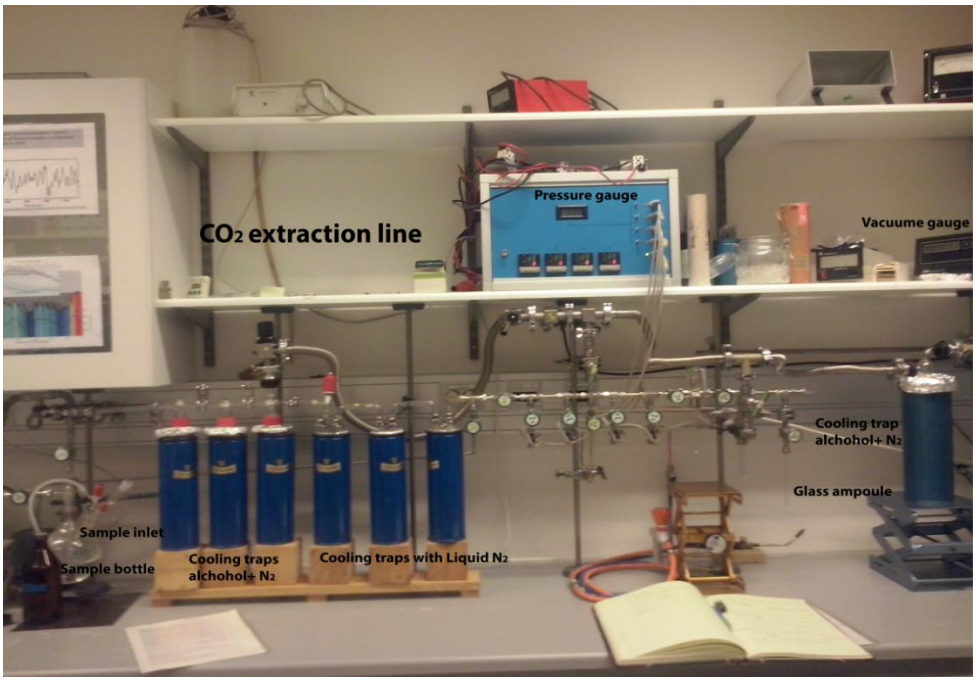

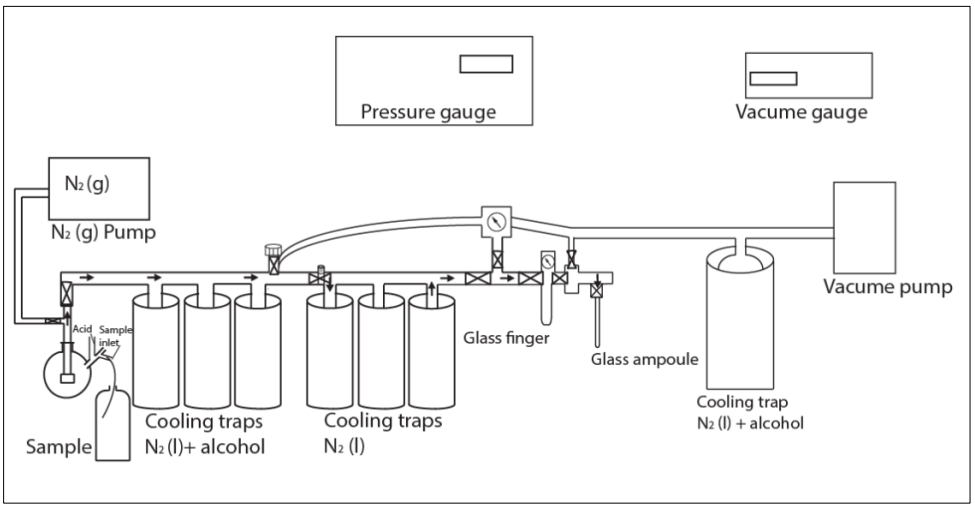

Figure 2 The CO_2 extraction line at the University of Iceland.

4 Geochemical modelling

Geochemical model calculations were carried out to gain further insight into CO_2-water-rock interaction and carbon isotope systematics. This involved calculation of aqueous speciation and mineral saturation states, isotope mixing model, reaction path modelling and reaction path isotope modelling. The calculations were carried out using the PHREEQC (Parkhurst and Appelo, 1999) and using home-made calculations routines.

4.1 Aqueous speciation and mineral saturation

Aqueous speciation and mineral saturation for the water samples were calculated with the aid of the PHREEQC program using the llnl.dat database (Parkhurst and Appelo, 1999). The database was updated to include some recent mineral solubility constants reported by Gysi and Stefánsson (2011).

Mineral saturation states were calculated from the expression,

$$SI = \log(Q/K)$$

where K is the equilibrium solubility constant for a particular mineral reaction and Q is the reaction quotient defined by,

$$Q = \prod a_i^{v_i}$$

where a_i is the activity of the i-the mineral or species and v_i is the respective reaction stoichiometric coefficient, which is positive for products and negative for reactants.

4.2 Isotope mixing model of Sveinbjörnsdóttir et al. (1995)

Sveinbjörnsdóttir et al. (1995) proposed a model for tracing the source of carbon in ground waters in Iceland using dissolved inorganic carbon concentration, $\delta^{13}C$ and boron. The model is referred here to as an isotope mixing model. In the model dissolved inorganic carbon concentrations and $\delta^{13}C$ are assumed to dependent on various sources and their contribution to the overall carbon content. The sources of carbon and $\delta^{13}C$ were assumed to be rock leaching, atmospheric CO_2 and organic matter. In the model the $\delta^{13}C^{atm}$ for the atmosphere was taken to be -7‰, the organic $\delta^{13}C^{org}$ was -25‰ and the $\delta^{13}C^{rock}$ rock value (basalt) was taken to be -4‰. The overall measured $\delta^{13}C$ in the ground water samples was then assumed to be equal to,

$$\delta^{13}C^{measured} = X^{atm}\delta^{13}C^{atm} + X^{rock}\delta^{13}C^{rock} + X^{organic}\delta^{13}C^{organic}$$

where X^{atm}, X^{rock} and $X^{organic}$ are the atmospheric, rock and organic fractions, respectively, and

$$X^{atm} + X^{rock} + X^{organic} = 1$$

Following Sveinbjörnsdóttir et al. (1995), the rock fraction, X^{rock}, may be calculated from the rock leached B in the water ($mB^{rock\ leached}$) as proposed by Arnórsson and Andrésdóttir (1995), the CO_2/B rock ratio and the measured CO_2 concentration in the samples (mCO_2), i.e.

$$X^{rock} = \frac{mB^{rock\ leached}\left(CO_2^{rock}/B^{rock}\right)}{mCO_2}$$

The atmospheric fraction, X^{atm}, may then be calculated combining the rock derived CO_2 fraction and the CO_2 isotope mass balance equation to give,

$$X^{atm} = \frac{\delta^{13}C^{measured} - \delta^{13}C^{organic} + X^{rock}\left(\delta^{13}C^{organic} - \delta^{13}C^{rock}\right)}{\delta^{13}C^{atm} - \delta^{13}C^{organic}}$$

and

$$X^{organic} = (1\text{-}X^{rock})\text{-}X^{atm}$$

For the calculations the $\delta^{13}C^{atm}$, $\delta^{13}C^{rock}$ and $\delta^{13}C^{organic}$ were taken from Sveinbjörnsdóttir et al. (1995), the average B^{rock} value for basalt was taken to be 1.2 ppm (Arnórsson and Andrésdóttir, 1995) and the average CO_2^{rock} in basalt was taken to be 70 ppm (Barry et al., 2014).

4.3 Reaction path modelling

Reaction path modelling was carried out to simulate the interactions of basalt with geothermal waters. Initial water composition was taken to be that of pure rainwater from Langjökull in equilibrium with atmospheric CO_2 or at higher concentrations. The rain water without elevated CO_2 concentration was then allowed to react with basaltic glass as a proxy for basalts in steps and the saturated secondary minerals in each step then allowed to precipitate. The composition of the basaltic glass, the starting solution and the secondary minerals incorporated in the calculations are given in Tables 1 to 3. The secondary minerals included are those commonly observed under weathering and low-temperature conditions of basalts and include oxides and hydroxides, clays, zeolites and carbonates. The chemical composition of the basaltic glass was taken from Gysi and Stefánsson (2012) but was modified to include C taken to be the average concentration of C in basaltic glass of 70 ppm Barry et al. (2014).

Table 1 Chemical composition of Stapafell glass used in model calculations.

Element	wt.%
SiO_2	48.29
Na_2O	2.01
K_2O	0.29
FeO_{tot}	10.47
Al_2O_3	14.47
MgO	8.45
CaO	12.2
TiO_2	1.58
MnO	0.19
CO_2	0.00729
Total	97.96
	mol
Si	1
Na	0.08
K	0.008
$Fe(II)_{tot}$	0.18
Al	0.35
Mg	0.26
Ca	0.27
Ti	0.02
Mn	0.003
C	0.0002

Table 2 Starting water composition used in the reaction path modelling.

Element	µmol/kg
Si	3.3
Na	61
K	1
Ca	0.7
Mg	6.7
Al	0.046
Fe	0
Cl	60.2
CO_2	160-114000
SO_4	0

Table 3 Minerals included in the reaction path and reaction path isotope simulations.

Mineral	Formula	25°C	100°C
Basaltic Glass	$K_{0.008}Na_{0.08}Ca_{0.27}Mg_{0.26}Mn_{0.003}Ti_{0.02}Fe_{0.181}Al_{0.35}Si_{1.0}C_{0.0002}O_{3.3294}$	x	x
Chalcedony	SiO_2	x	x
Ferrihydrite	$Fe(OH)_3$	x	
Gibbsite	$Al(OH)_3$	x	
Calcite	$CaCO_3$	x	x
Dolomite	$(Ca,Mg)CO_3$	x	x
Siderite	$FeCO_3$	x	x
Magnesite	$MgCO_3$	x	x
Mg-Fe carbonates	$(Fe,Mg)CO_3$	x	x
Mg-Fe smectite	$Na_{0.04}K_{0.10}Ca_{0.21}Mg_{1.44}Fe_{1.78}Al_{1.00}Si_{3.00}O_{10}(OH)_2$	x	x
Clinochlore	$Mg_5Al_2Si_3O_{10}(OH)_8$		x
Celadonite	$KMgAlSi_4O_{10}(OH)_2$		x
Fe-Celadonite	$KFeAlSi_4O_{10}(OH)_2$		x
Chabazite	$CaAl_2Si_4O_{12}\cdot 6H_2O$	x	x
Analcime	$Na_{0.96}Al_{0.96}Si_{2.04}O_6\cdot 1.02H_2O$	x	x
Heulandite	$CaAl_2Si_7O_{18}\cdot 6H_2O$	x	x
Mesolite	$Ca_{0.667}Na_{0.666}Al_2Si_3O_{10}\cdot 2.667H_2O$	x	x
Mordenite	$Ca_{0.5}AlSi_5O_{12}\cdot 4H_2O$	x	x
Stilbite	$Ca_2NaAl_5Si_{13}O_{36}\cdot 16H_2O$	x	x
Thomsonite	$Ca_2NaAl_5Si_5O_{20}\cdot 6H_2O$	x	x
Natrolite	$Na_2Al_2Si_3O_{10}\cdot 2H_2O$	x	x

4.4 Reaction path isotope modelling

The reaction path simulations were expanded to include carbon isotope fractionation upon reaction progress. For each reaction step, the isotope systematics was calculated based on relative mass distribution of carbon species and carbonate minerals assuming equilibrium. In the reaction path isotope model three aqueous species were included, CO_2(aq), HCO_3^- and CO_3^{2-} and that the carbonate formed were taken to be represented by calcite. At present more aqueous species and carbonate minerals cannot be included into the model because of limit data available for carbon isotope fractionation discussed in the next section. Further, the system is assumed to be thermodynamically closed, i.e. there is no loss of total mass in the system, only mass transfer from one species to the other and between phase. The source of carbon and the isotope carbon content is then assumed to be the source water and the primary rock taken to be basalt.

The reaction path isotope model involves essentially two steps. The first step is a conventional reaction path modelling whereas rock is added in steps into the source water and fully dissolved, aqueous speciation calculated and minerals that become saturated allowed to form. This part of the reaction path isotope model is essentially the reaction path model described previously and was conducted with the aid of the PHREEQC program (Parkhurst and Appelo, 1999). From the reaction path calculation the mole distribution of dissolved carbonate species is obtained as well as mass of carbonates formed as a function of reaction progress (ξ). Here the reaction progress is taken as the moles of basalt dissolved in kg of water.

The reactions involved for carbon in the reaction path isotope geochemical model were,

$$CO_2(aq) + H_2O = H^+ + HCO_3^-$$
$$HCO_3^- = H^+ + CO_3^{2-}$$
$$CaCO_3(s) + 2H^+ = Ca^{2+} + CO_2(aq) + H_2O$$
$$basalt + 1.13H^+ + 2.199H_2O = solutes + 0.0002CO_2(aq)$$

in addition to various secondary minerals allowed to form as discussed previously.

The fractionation between the various aqueous species and calcite is defined according to,

$$\alpha_{HCO_3-CO_2(aq)} = \frac{1000 + \delta^{13}C_{HCO_3^-}}{1000 + \delta^{13}C_{CO_2(aq)}}$$

$$\alpha_{CO_3-CO_2(aq)} = \frac{1000 + \delta^{13}C_{CO_3^{2-}}}{1000 + \delta^{13}C_{CO_2(aq)}}$$

$$\alpha_{calcite-CO_2(aq)} = \frac{1000 + \delta^{13}C_{calcite}}{1000 + \delta^{13}C_{CO_2(aq)}}$$

where $\alpha_{HCO_3-CO_2(aq)}$, $\alpha_{CO_3-CO_2(aq)}$ and $\alpha_{calcite-CO_2(aq)}$ are the respective equilibrium fractionation factors and $\delta^{13}C_i$ are the isotope values for the appropriated aqueous species and calcite.

The total $\delta^{13}C$ isotope composition of the system ($\delta^{13}C^{total}$) was taken to be that of the initial water and the dissolved basalt in the appropriated fraction,

$$\delta^{13}C^{systems} = x_{CO_2}^{source\ water}\delta^{13}C^{source\ water} + x_{CO_2}^{rock}\delta^{13}C^{rock}$$

where $x_{CO_2}^{source\ water}$ and $x_{CO_2}^{rock}$ are the mole ΣCO_2 fraction in the water derived from the initial source water and the source rock (taken to be basalt) defined by,

$$x_{CO_2}^{source\ water} = \frac{m_{CO_2}^{source\ water}}{m_{CO_2}^{source\ water} + m_{CO_2}^{rock}}$$

$$x_{CO_2}^{rock} = \frac{m_{CO_2}^{rock}}{m_{CO_2}^{source\ water} + m_{CO_2}^{rock}}$$

where $m_{CO_2}^{source\ water}$ and $m_{CO_2}^{rock}$ are the molal CO_2 concentrations derived from the source water and the rock, respectively. The rock derived concentration of ΣCO_2 is derived from the moles of rock (basalt) dissolved in kg of water, i.e. the extent of reaction (ξ) and the mole fraction of CO_2 in the basalt ($x_{CO_2}^{basalt}$),

$$m_{CO_2}^{rock} = x_{CO_2}^{basalt}\xi$$

Assuming the system to be closed, i.e. no changes in total mass within the system, it follows that,

$$m_C^{system} = m_{CO_2}^{source\ water} + m_{CO_2}^{rock} = m_{CO_2(aq)} + m_{HCO_3^-} + m_{CO_3^{2-}} + m_{calcite}$$

where m_i are the mole concentrations of the i-the component, aqueous species or minerals. With respect to carbon isotopes for a closed system we have,

$$\delta^{13}C^{system} = x_{CO_2(aq)}\delta^{13}C_{CO_2(aq)} + x_{HCO_3^-}\delta^{13}C_{HCO_3^-} + x_{CO_3^{2-}}\delta^{13}C_{CO_3^{2-}} + x_{calcite}\delta^{13}C_{calcite}$$

where x_i are the appropriated mole fractions of CO_2(aq), HCO_3^-, CO_3^{2-} and calcite that varies as a function of reaction progress. Combining the fractionation factors and the mass conservation isotope formula together one obtains,

$$\delta^{13}C^{system} = x_{CO_2(aq)}\delta^{13}C_{CO_2(aq)} + x_{HCO_3^-}\delta^{13}C_{HCO_3^-} + x_{CO_3^{2-}}\delta^{13}C_{CO_3^{2-}} + x_{calcite}\delta^{13}C_{calcite}$$

and solving for CO_2(aq)

$$\begin{aligned}\delta^{13}C^{system} = \quad & x_{CO_2(aq)}\delta^{13}C_{CO_2(aq)} \\ & + x_{HCO_3^-}\left(\left(\alpha_{\mathrm{HCO_3-CO_2(aq)}}\left(1000 + \delta^{13}\mathrm{C_{CO_2(aq)}}\right)\right) - 1000\right) \\ & + x_{CO_3^{2-}}\left(\left(\alpha_{\mathrm{CO_3-CO_2(aq)}}\left(1000 + \delta^{13}\mathrm{C_{CO_2(aq)}}\right)\right) - 1000\right) \\ & + x_{calcite}\left(\left(\alpha_{\mathrm{calcite-CO_2(aq)}}\left(1000 + \delta^{13}\mathrm{C_{CO_2(aq)}}\right)\right) - 1000\right)\end{aligned}$$

Knowing the isotope fractionation factors, $\delta^{13}C^{system}$ and the mole fraction of the appropriated aqueous species and calcite, the isotope values for CO_2(aq), HCO_3^-, CO_3^{2-} and calcite were calculated using non-linear regression.

The initial conditions of the reaction path isotope simulations are summarized in Table 4. The initial water composition take to be meteoric water in equilibrium with atmospheric CO_2 (7 ppm) or elevated CO_2 source (5000 ppm) with $\delta^{13}C$ of -7 and -3‰, respectively. The latter value of -3‰ was chosen arbitrary to possibly explain waters with elevated CO_2 concentrations and heavy $\delta^{13}C$ values. The initial concentration of the CO_2 in the basalts was taken to be 70 ppm (Barry et al., 2014). The recently measured $\delta^{13}C$ values for rocks vary over a large interval (Barry et al., 2014). A value of $\delta^{13}C$ for the basalts was taken to be -7‰. This value is somewhat higher than the average basalt value of Barry et al. (2014), however, it is the same as the meteoric value and it follows that the source carbon isotope value is constant in the model and the carbon isotope systematics only depend on the reaction path isotope modeling. Lastly, for the reaction path isotope modelling the equilibrium carbon isotope fractionation factors are needed. These were revised in this study, this discussed below.

Table 4 The initial conditions of the reaction path and reaction path isotope simulations

	Reaction path	Reaction path isotope
t (°C)	25-100°C	25-100°C
ξ basalt	0-1 mol/kg solution	0-1 mol/kg solution
ξ steps	1000	1000
$m_{CO_2}^{source\ water}$	7 ppm	7-5000 ppm
$m_{CO_2}^{rock}$	70 ppm	70 ppm
$\delta^{13}C^{rock}$		-7 ‰
$\delta^{13}C^{source\ water}$		-3 and -7 ‰

4.5 Carbon isotope fractionation factors

Equilibrium isotope fraction has been experimentally determined between CO_2(g), CO_2(aq), HCO_3^-, CO_3^{2-} and calcite,

$$\alpha_{CO_2(aq)-CO_2(g)} = \frac{1000 + \delta^{13}C_{CO_2(aq)}}{1000 + \delta^{13}C_{CO_2(g)}}$$

$$\alpha_{HCO_3-CO_2(g)} = \frac{1000 + \delta^{13}C_{HCO_3^-}}{1000 + \delta^{13}C_{CO_2(g)}}$$

$$\alpha_{CO_3-CO_2(g)} = \frac{1000 + \delta^{13}C_{CO_3^{2-}}}{1000 + \delta^{13}C_{CO_2(g)}}$$

$$\alpha_{calcite-CO_2(g)} = \frac{1000 + \delta^{13}C_{calcite}}{1000 + \delta^{13}C_{CO_2(g)}}$$

$$\alpha_{calcite-HCO_3} = \frac{1000 + \delta^{13}C_{calcite}}{1000 + \delta^{13}C_{HCO_3^-}}$$

The α value is generally very close to one. Therefore α is commonly reported as $10^3 \ln\alpha$ or $\varepsilon = (\alpha\text{-}1)10^3$. The two give almost identical values, however, to be consistent the isotope fractionation is given in terms of $10^3 \ln\alpha$ in this study and all literature values reported as ε were converted to $10^3 \ln\alpha$. Smoothed temperature dependence fractionation factors were obtained by fitting the experimental data to a function of the form,

$$10^3 \ln\alpha = a/T + b$$

The $\alpha_{CO_2(aq)-CO_2(g)}$ has been experimetally determined by Vogel et al. (1970), Zhang et al (1995) and Myrttinen et al. (2014) from 0 to 120°C. The values are in fair agreement, with differences of $10^3 \ln\alpha$ up to 0.2. The experimental values are plotted in Figure 3 together with the temperature function obtained in this study by fitting all the data, given in Table 5.

The $\alpha_{HCO_3-CO_2(g)}$ has been experimentally determined by Zhang et al. (1995), Malinin et al. (1967), Szaran (1997), Emrich et al. (1970), Mook et al. (1974), Deuser and Degens (1967) from 0 to 286 °C. At temperatures <100°C there is general good agreement between various results with the exception of Deuser and Degens (1967) that are systematically lower than others. At 100-300°C the results of Malinin et al. (1967) are extensive but somewhat scattered. They are however consistent with extrapolation of low-temperature data to higher temperatures. The experimental values are plotted in Figure 3 together with the temperature function obtained in this study by fitting all the data, given in Table 5.

The $\alpha_{CO_3-CO_2(g)}$ has been experimentally determined by Halas et al. (1997) and Zhang et al. (1995) at 0 to 80°C. The two datasets are in reasonable agreement at ambient temperature, however, the temperature effects of the two studies is somewhat different resulting in variable values extrapolated to elevated temperatures. Here, both datasets were included in the fit to obtain temperature function for $10^3 \ln\alpha_{CO_3-CO_2(g)}$ as a function of temperature. The experimental values are plotted in Figure 3 together with the temperature function obtained in this study by fitting all the data, given in Table 5.

The $\alpha_{calcite-CO_2(g)}$ has been experimentally determined by Emrich et al. (1970) and Romanek et al. (1992) and also estimated by Bottinga (1969). The experimental values range in temperature from 10 to 50°C. Our fit included the data of Emrich et al. (1970) and Romanek et al. (1992) and extrapolation to elevated temperatures. The comparison of the present study with the estimation of Bottinga (1969) is reasonable to ~200°C but the two deviate at higher temperatures. The experimental values are plotted in Figure 3 together with the temperature function obtained in this study by fitting all the data, given in Table 5.

The $\alpha_{calcite-HCO_3}$ has been experimentally determined by Rubinson and Clayton (1969) and Romanek et al. (1992) at 10 to 40°C. The data are spread over conservable range or four $10^3 \ln\alpha$ units. In the case of $\alpha_{calcite-HCO_3}$ the temperature functions were obtained from the $\alpha_{calcite-CO_2(g)}$ and $\alpha_{HCO_3-CO_2(g)}$ smoothed functions rather than direct fit. In this way a consistent dataset is obtained as well as the scatter of the α_{cc-HCO_3} does not contribute to the extrapolation. The experimental values are plotted in Figure 3 together with the temperature function obtained in this study by fitting all the data, given in Table 5. As can be seen the calculated smoothed fractionation factors based on the fitted $\alpha_{calcite-CO_2(g)}$ and $\alpha_{HCO_3-CO_2(g)}$ smoothed functions are in very good agreement with the experimental values.

Based on the various smoothed fractionation factors and the principle of additivity, a full set of fractionation factors between various aqueous species and calcite were obtained. The functions for calculations of the smoothed fractionation factors are given in Table 5. These smoothed functions are the bases for calculation of equilibrium isotope fractionation between aqueous inorganic carbon species and calcite.

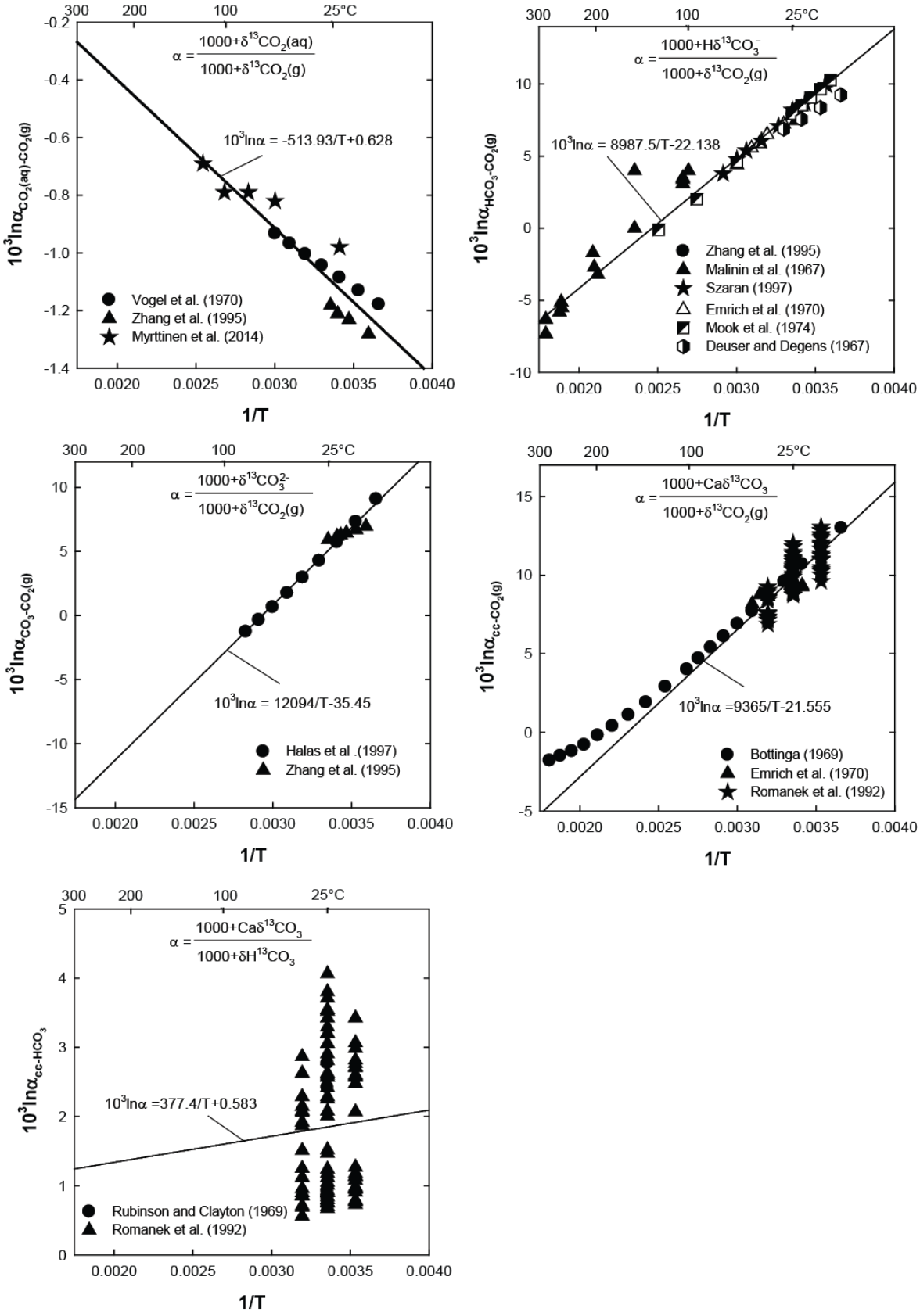

Figure 3 Isotope fractionation factors as a function of 1/T in Kelvin. Shown are various experimentally derived values together with the fit obtained in this study.

Table 5 Carbon isotope fractionation factors derived in this study.

Reaction	Equilibrium fractionation function $10^3 \ln\alpha$ Valid at 0-300°C
cc-HCO_3	377.4/T+0.583
cc-CO_2(g)	9364.9/T-21.555
cc-CO_2(aq)	9878.83/T-22.183
CO_2(aq) - CO_2(g)	-513.93/T+0.628
HCO_3 - CO_2(g)	8987.5/T-22.138
CO_3 - CO_2(g)	12094/T-35.45
HCO_3-CO_2(aq)	9501.43/T-22.766
CO_3-CO_2(aq)	12607.93/T-36.078
HCO_3 - CO_3	-3106.5/T+13.312

5 Water chemistry and carbon isotope systematics

The major elemental composition of the water samples is given in Table 6. The sampling temperature ranged from 3°C to 97°C and the pH range varies from 6.18 to 10.15 at room temperature. Based on the anion distribution the waters were divided into three groups: Thermal NaCl waters, thermal and non-thermal carbonate waters and non-thermal waters (Fig. 4). Carbonate waters have elevated CO_2 concentration and mildly acid pH. Iron, Mg, Ca and K concentrations are order of magnitude higher compared to NaCl waters and non-thermal waters. NaCl waters have a pH ranging from near neutral to slightly alkaline. Chloride is the dominant anion and Na and Si the dominant cations. The concentrations of many metals are low including Mg, Fe and Al. The temperatures range from ambient to boiling. Non-thermal waters represent cold ground- and surface water and are generally low in dissolved elements. The dissolved inorganic carbon (CO_2) concentration in the water samples ranged from 1.8 to 2853 ppm. In non-thermal waters the concentration was the lowest in general or 8.7-19.4 ppm, followed by NaCl water with 1.8-381 ppm and highest for CO_2 waters 1782-2853 ppm.

The carbon isotope systematics of the water samples are given in Table 6 and plotted as a function of temperature, pH, ΣCO_2 and Cl in Figure 5. The carbon isotopes were found to be in the range $\delta^{13}C$ -1.46 to -13.96‰. In non-thermal waters $\delta^{13}C$ was -9.42 to -4.91 ‰, for NaCl water $\delta^{13}C$ was -13.96 to -1.46 ‰ and for CO_2 waters $\delta^{13}C$ was -4.15 to -3.62 ‰. No obvious trend was observed between $\delta^{13}C$, temperature and Cl concentration. However, $\delta^{13}C$ is observed to increase with increasing CO_2 concentration and decrease with increasing pH.

Figure 6 shows the $\delta^{13}C$ relation with CO_2 for natural waters in Iceland reported in this study, as well as by Sveinbjörnsdóttir et al. (1995) and Barry et al. (2014). Values for basalts reported by Barry et al. (2014) and various end-member components including organic matter, atmosphere, seawater and the mantle are also shown (Hoefs, 1997). Waters, containing low concentrations of dissolved CO_2, about <70 ppm, have values that are very close to Icelandic basalts, suggesting a possible rock and atmospheric origin. With increasing CO_2 concentration, there are two trends observed, one showing increased negative $\delta^{13}C$ with decreasing CO_2 concentration and the other showing positive increase in $\delta^{13}C$ (closer to 0) with increasing CO_2 concentration and then a relatively steady value of -4 to -2 ‰ above 100 ppm CO_2. The former trend suggests an organic CO_2 source whereas the latter suggest a possible mantle source or even another source slightly more positive than the mantle. Carbonates like calcite are known to have heavier $\delta^{13}C$ than the mantle, suggesting a possible carbonate source of the elevated CO_2 and heavy $\delta^{13}C$ waters (Hoefs, 1997). The possible source and reactions of CO_2 in low-temperature geothermal waters in Iceland are explored below.

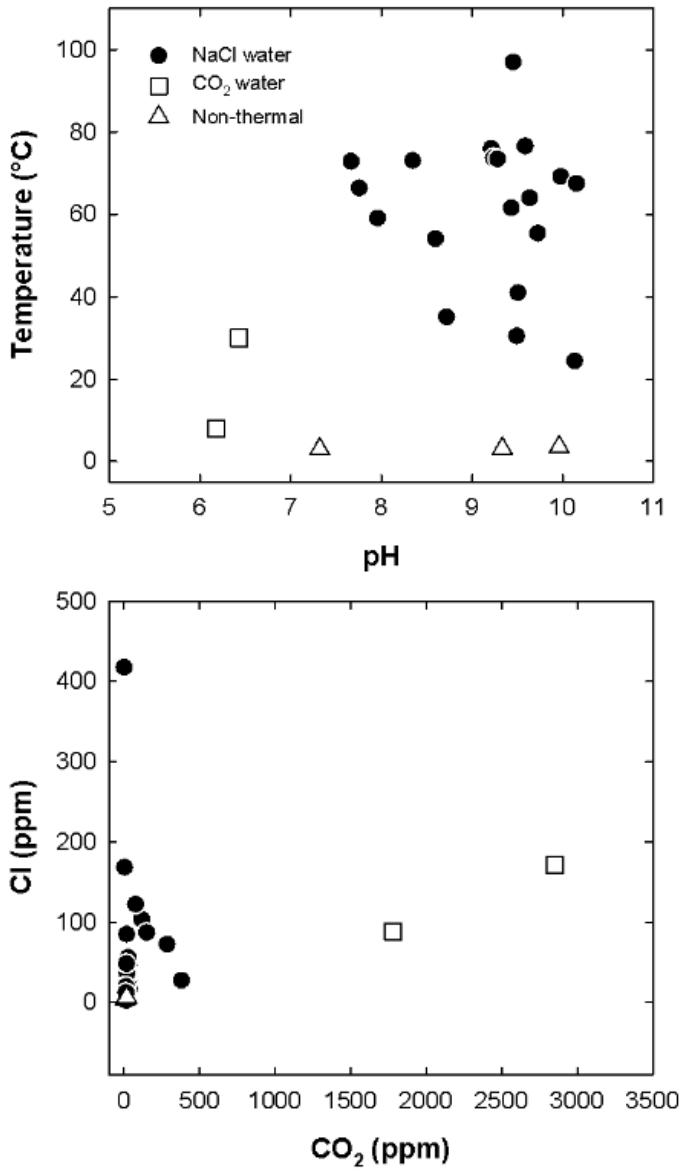

Figure 4 The relationship between pH and temperature, and CO_2 and Cl in the sampled waters.

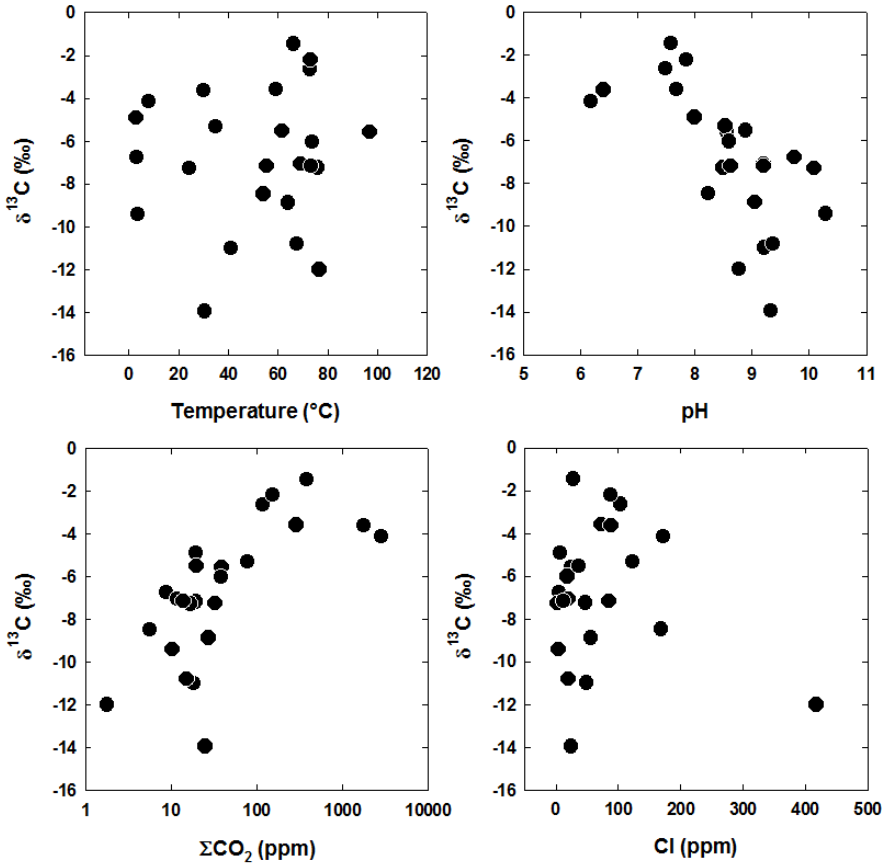

Figure 5 The relationship between $\delta^{13}C$ and temperature, pH, CO_2, and Cl.

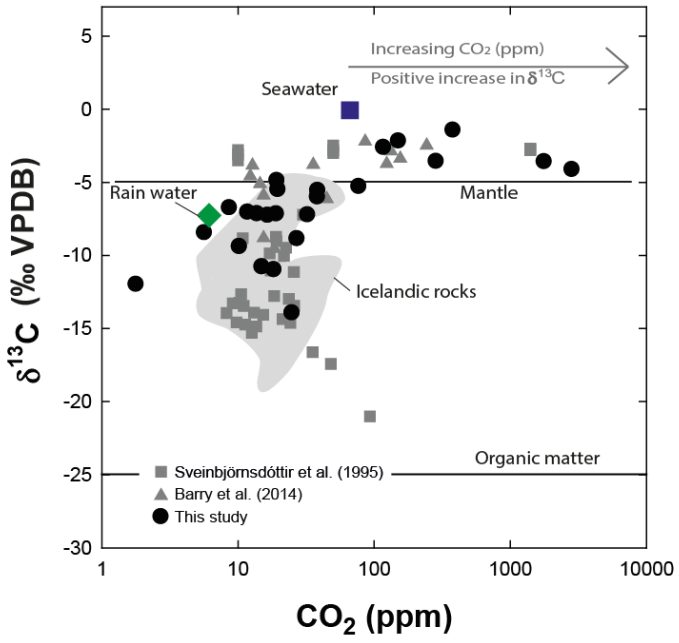

Figure 6 The relationship between $\delta^{13}C$ and CO_2 for sampled fluids in Iceland and rocks together with some reference samples.

Table 6 Chemical analysis of geothermal waters

Sample #	Location	t°C	pH	/	°C	B ppm	SiO_2 ppm	Na ppm	K ppm	Ca ppm	Mg ppm	Fe ppm	Al ppm	CO_2 ppm	Cl ppm	SO_4 ppm	H_2S ppm	$\delta^{13}C$ (‰)
12-RK-1	Vaðmálahver	97	9.45	/	19.7	0.392	150.9	82.0	2.229	1.97	0.016	0.018	0.176	38.74	24.90	53.47	1.629	-5.59
12-RK-2	Spóastaðir	76	9.21	/	20	0.293	103.3	83.6	1.926	4.05	0.021	0.016	0.038	32.67	47.75	50.39	1.146	-7.26
12-RK-3	Ljósuár	3.5	9.96	/	20.3	0.007	13.82	12.1	0.110	2.50	0.085	0.007	0.039	10.30	4.246	1.30	0.000	-9.42
12-RK-4	Vellankatla	3.1	9.33	/	20.6	0.006	14.47	6.49	0.463	2.84	0.922	0.011	0.040	8.709	4.422	1.18	0.000	-6.77
13-RK-5	Eyvík	72.9	7.67	/	21.9	0.164	170.9	156	5.517	4.60	0.058	0.065	0.107	117.7	103.8	54.2	0.148	-2.64
13-RK-6	Núpar	35.1	8.72	/	19.3	0.246	80.25	133	2.815	4.67	0.249	0.033	0.031	77.53	122.5	29.7	0.002	-5.32
13-RK-7	Neðri-Dalur	66.4	7.76	/	20.6	0.205	177.4	211	38.74	10.4	1.055	0.055	0.027	381.3	27.77	15.4	0.020	-1.46
13-RK-8	Húsatóftir	54.1	8.60	/	21.6	0.224	72.33	151	2.351	12.9	0.006	0.015	0.069	5.702	168.5	65.0	0.006	-8.48
13-RK-9	Sogið	3.0	7.32	/	21.0	0.009	10.92	9.35	0.721	4.37	1.563	0.041	0.022	19.44	6.821	2.61	0.000	-4.91
13-RK-10	Gýgjarhóll	59.1	7.96	/	21.1	0.423	155.0	235	15.27	6.73	0.783	0.052	0.032	287.1	72.72	82.9	0.146	-3.6
13-RK-11	Efstaland	64	9.64	/	21.3	0.196	87.64	81.2	1.31	3.07	0.088	0.008	0.045	27.33	56.32	28.1	0.167	-8.89
13-RK-12	Marteinslaug	73.1	8.35	/	21.4	0.750	303.6	175	12.96	5.58	0.276	0.028	0.056	152.0	87.22	61.7	0.139	-2.2
13-RK-13	Oddgeirshólar	76.6	9.59	/	21.4	0.152	67.57	273	4.77	53.7	0.016	0.028	0.053	1.794	417.8	88.9	0.050	-12.01
13-RK-14	Reykir	73.7	9.24	/	21.4	0.233	153.1	74.6	2.20	2.48	0.029	0.004	0.064	38.57	18.38	51.8	0.435	-6.03
13-RK-15	Krosslaug	30.5	9.49	/	21.4	0.229	67.17	69.4	0.794	3.44	0.011	0.004	0.022	25.09	24.75	58.9	0.052	-13.96
13-RK-16	Húsafell	61.6	9.43	/	21.8	0.454	82.53	92.6	1.745	4.78	0.009	0.008	0.063	19.74	36.76	68.8	0.167	-5.52
13-RK-17	Runnar	41	9.51	/	22.4	0.227	106.7	84.5	2.078	3.11	0.006	0.030	0.089	18.47	48.43	52.6	0.045	-11
13-RK-18	Sjávarborg	69.2	9.98	/	20.7	0.160	68.78	55.6	0.782	3.33	0.002	0.004	0.074	11.86	20.17	37.3	0.433	-7.07
13-RK-19	Hofsvellir	73.5	9.28	/	21.1	1.399	109.8	118	2.310	4.94	0.003	0.005	0.040	19.26	85.20	85.9	0.328	-7.19
13-RK-20	Varmilækur	67.5	10.15	/	21.3	0.309	87.98	61.1	0.718	1.65	0.011	0.005	0.133	15.08	20.12	19.2	0.072	-10.81
13-RK-21	Víðivellir	24.4	10.13	/	21.4	0.070	34.39	27.2	0.123	1.65	0.019	0.009	0.052	16.63	2.642	2.23	0.012	-7.29
13-RK-22	Laugar	55.4	9.72	/	22.1	0.042	63.95	68.7	0.613	3.71	0.025	0.070	0.072	13.90	12.40	51.2	0.385	-7.18
13-RK-23	Ölkelda	8.0	6.18	/	8.0	0.788	79.35	537	20.44	204	45.19	7.132	0.026	2853	171.6	99.6	0.007	-4.15
13-RK-24	Lýsuhóll	30	6.43	/	22	0.527	142.9	467	25.67	148	43.83	3.121	0.014	1782	88.57	50.3	0.009	-3.62

6 Geochemistry of CO_2 and the source and reactions of carbon in low-temperature geothermal systems

The geochemistry of CO_2 and its sources and reactions in low-temperature geothermal waters in Iceland was studied by three approaches. Firstly, the distribution and reactions of aqueous species of inorganic dissolved carbon was examined together with the carbonate mineral saturation state. The information gained from such calculations are useful to qualitatively assess the possible reaction occurring as well as if carbonate minerals may possible be forming within the surface- and groundwater systems under various conditions, like temperature and pH. Secondly, a component mixing model first reported by Sveinbjörnsdóttir et al. (1995) was applied. In this model, CO_2 concentrations together with $\delta^{13}C$ values for various end-members (rocks, atmosphere and organic matter) are used to assess the source of CO_2 in the waters. Thirdly, a reaction path and reaction path isotope model was developed and applied to simulate carbonate chemistry, carbonate mineral formation and isotope systematics upon progressive water-rock interaction and including various and possible end-member carbon sources. These were then compared with the measured carbon and $\delta^{13}C$ in the low-temperature waters.

6.1 Aqueous speciation of dissolved inorganic carbon

The results of the aqueous speciation calculations are shown in Figure 7. In mildly acid to alkaline waters, CO_2(aq), HCO_3^- and CO_3^{2-} were found to predominate. Ion pairs, particularly Ca, Mg and Na bicarbonate and carbonate ions pairs were also observed to be important. The calculations were conducted with the aid of the PHREEQC program and using the llnl.dat database (Parkhurst and Appelo, 1999). The outcome of the aqueous speciation calculations largely depends on the thermodynamic database used and the results should therefore be viewed with some care. However, carbonic acid and its ionized forms seem to be the most important aqueous reactions in non-thermal and low-temperature geothermal waters in Iceland.

The potential of mineral formation may be assessed by looking at the various mineral saturation states. The saturation state with respect to calcite, dolomite, siderite and magnesite as a function of pH is shown in Figure 8. These represent end-member carbonate minerals, however, other types including Mg-Fe solid solutions and ankerite solid solutions may also be of importance but these have not been included here.

Most samples were observed to be close to calcite saturation. The same is true with respect to dolomite for the mildly acid and neutral waters having elevated CO_2 concentration. On the contrary almost all waters were calculated to be siderite undersaturated and all to be magnesite undersaturated. This suggest that calcite is likely to be the predominant carbonate forming mineral in non-thermal and low-temperature geothermal waters in Iceland and the existence of other carbonates, at least in large quantities, is unlikely. This is in line with observations on naturally altered rocks, where

calcite is often identified among the alteration product whereas other carbonates are very rarely observed (e.g. Mehegan et al., 1982; Neuhoff et al, 1999; Ólafsson et al., 2005). On the contrary, Gysi and Stefánsson (2011) observed experimentally that calcite together with Mg-Fe carbonates form in waters of high CO_2 concentrations and mildly acid pH and such solid solutions may possibly predominate the carbonate mineralization under such conditions at <100°C.

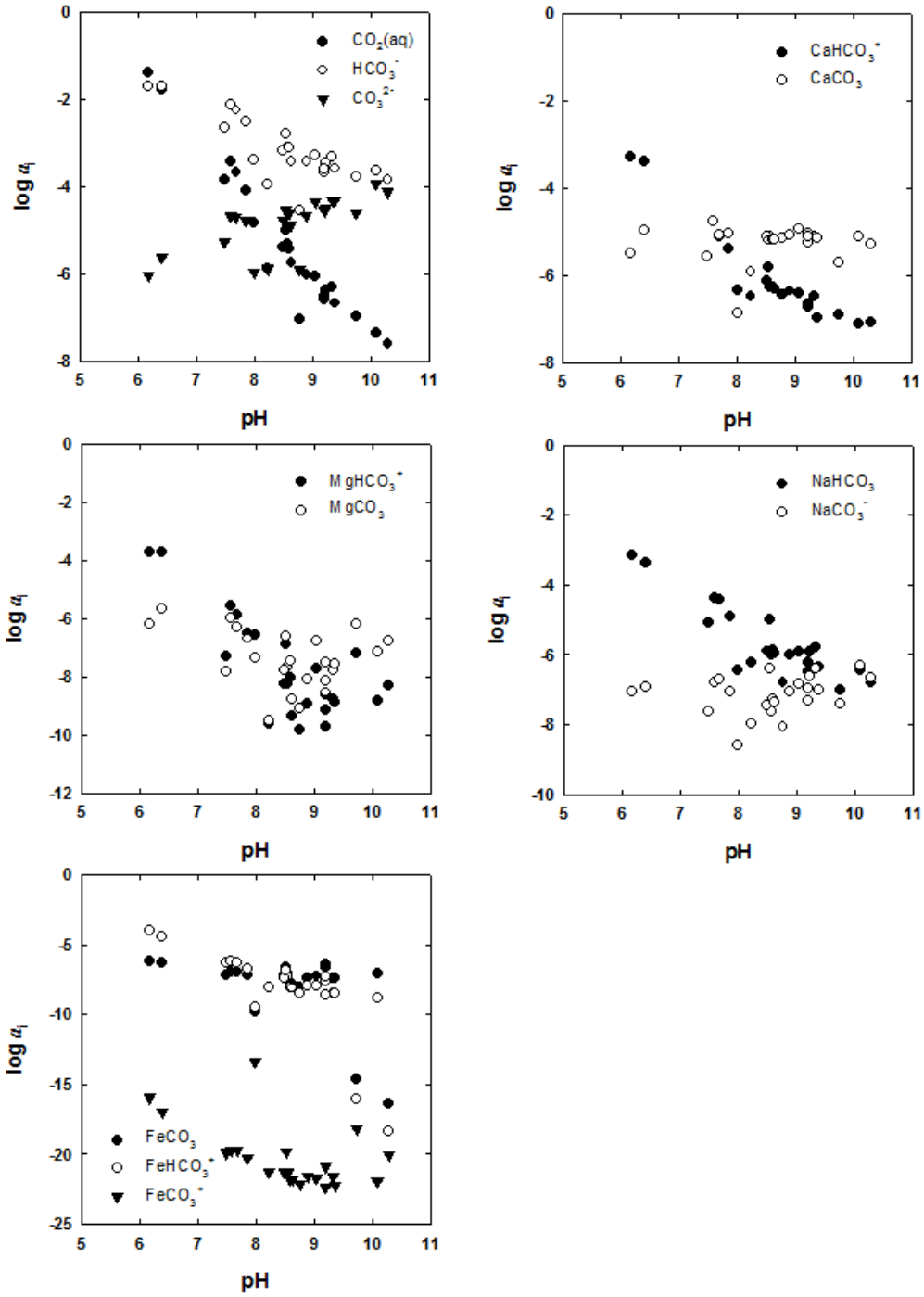

Figure 7 Aqueous speciation distribution of CO_2 containing aqueous species in the water samples.

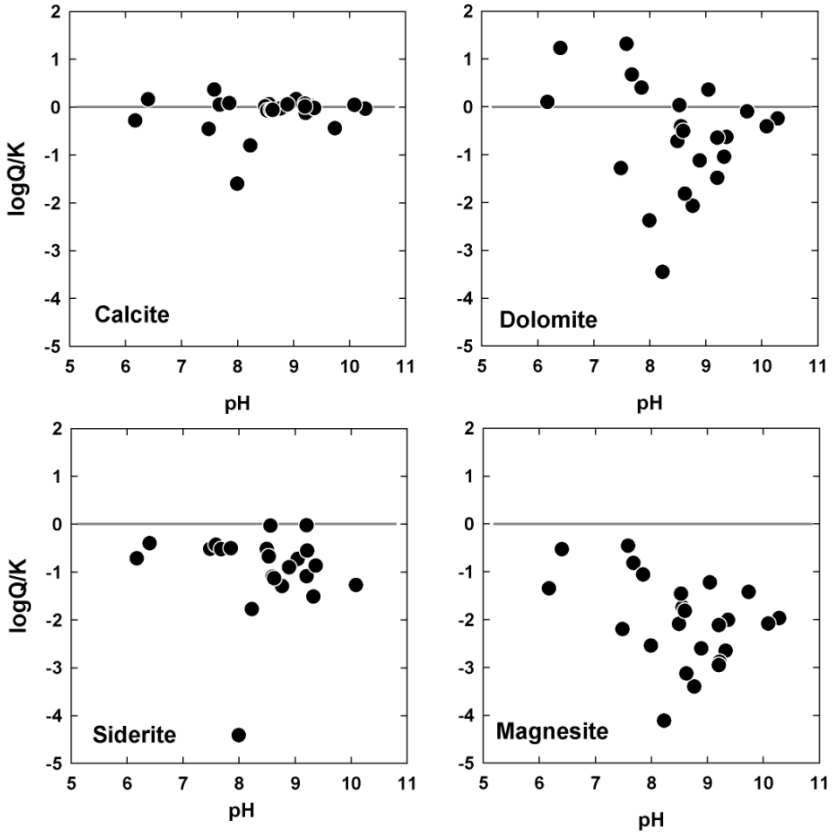

Figure 8 Mineral saturation states with respect to common carbonate minerals.

6.2 CO_2 source in groundwaters and the mixing model proposed by Sveinbjörnsdóttir et al. (1995)

The source of elements and isotopes is sometimes assumed to be controlled predominantly by the input from various sources. In the case of dissolved inorganic carbon and carbon isotopes Sveinbjörnsdóttir et al. (1995) proposed a model for tracing the source of carbon in groundwaters in Iceland using dissolved inorganic carbon concentration in the waters, $\delta^{13}C$ and boron. The detailed model setup, including all equations of importance was summarized in section 4.2. In the model, three sources of carbon and carbon isotopes are assumed to exist, i.e. rock leaching, atmospheric CO_2 and organic matter. The natural groundwaters are then assumed to be a mixture of these end-members.

The model proposed by Sveinbjörnsdóttir et al. (1995) was used to calculate the fraction of various sources contributing to the CO_2 and $\delta^{13}C$ in the water sampled in this study. The values obtained are reported in Table 7. The results indicate that the source of CO_2 in the low-temperature groundwater in Iceland range from being entirely rock derived, to entirely atmospheric derived to largely organically derived. However, 15 samples out of the 24 samples in total have either some negative CO_2 source values and/or source values greater than 1.0. This suggests that the simple source model of Sveinbjörnsdóttir et al. (1995) may be over simplified, at least in some cases, in estimating the source and reactions of CO_2 in natural waters in Iceland.

There may be at least three reasons for these observations. Firstly, the CO_2 concentrations and $\delta^{13}C$ values in basalt cannot be assumed to be represented by a single value, in fact the range of concentrations is very large from 16.5 to 273.3 ppm and -27.7 to -3.6 ‰, respectively (Barry et al., 2014), whereas in the model it was set to a value of 70 ppm and -4 ‰. Secondly, CO_2 may have at least five sources including atmospheric, rock derived, organic, marine and carbonate CO_2 but not only three as is assumed in the model. Thirdly, progressive water-rock interaction and aqueous speciation may influence the aqueous carbonate concentration and $\delta^{13}C$ systematics, but it is not only being controlled by the properties of the various sources. It is therefore concluded that the mixing model proposed by Sveinbjörnsdóttir et al. (1995) may be unrealistic in determining the source and reactions of CO_2 in low-temperature geothermal waters.

Table 7 The source of CO_2 in the water samples according to the model proposed by Sveinbjörnsdóttir et al. (1995).

#	Location	CO_2 source		
		X^{rock}	X^{atm}	X^{org}
12-RK-1	Vaðmálahver	0.59	0.39	0.02
12-RK-2	Spóastaðir	0.52	0.38	0.10
12-RK-3	Ljósuár	0.04	0.82	0.14
12-RK-4	Vellankatla	0.03	0.98	-0.01
13-RK-5	Eyvík	0.07	1.16	-0.23
13-RK-6	Núpar	0.17	0.90	-0.07
13-RK-7	Neðri-Dalur	0.03	1.27	-0.30
13-RK-8	Húsatóftir	1.93	-1.34	0.40
13-RK-9	Sogið	0.02	1.09	-0.11
13-RK-10	Gýgjarhóll	0.08	1.09	-0.17
13-RK-11	Efstaland	0.40	0.43	0.17
13-RK-12	Marteinslaug	0.29	0.93	-0.22
13-RK-13	Oddgeirshólar	1.85	-1.43	0.59
13-RK-14	Reykir	0.35	0.64	0.00
13-RK-15	Krosslaug	0.53	-0.01	0.48
13-RK-16	Húsafell	1.34	-0.48	0.14
13-RK-17	Runnar	0.70	-0.04	0.34
13-RK-18	Sjávarborg	0.78	0.09	0.13
13-RK-19	Hofsvellir	4.24	-3.95	0.72
13-RK-20	Varmilækur	1.20	-0.61	0.41
13-RK-21	Víðivellir	0.25	0.70	0.06
13-RK-22	Laugar	0.17	0.80	0.04
13-RK-23	Ölkelda	0.02	1.14	-0.16
13-RK-24	Lýsuhóll	0.02	1.17	-0.18

6.3 CO_2 source in groundwaters and reaction path modelling

From the geochemical perspective the source of carbon and carbon isotopes in natural waters may be influenced by various factors. Firstly, the source of carbon is important, possible sources being atmospheric or rain water, rock dissolution of either primary and/or secondary phases, seawater and organic source. Secondly, mixing between two or more waters having different carbon concentration and isotope composition may also be of importance. Thirdly, progressive water-rock interaction may change the carbon content and isotope systematics of the various phases and components involved, for example through rock dissolution and carbonate mineral formation. Fourthly, aqueous speciation may simultaneously influence the concentrations, mineral solubilities, and isotope fractionation between various phases and components in the system, aqueous speciation depending on for example pH.

In order to study possible variations in carbon concentrations and carbon isotope systematics, a geochemical model was developed which takes into account the possible sources and reactions of carbon and carbon isotopes, upon progressive dissolution of primary rocks and formation of carbonates. The model is described in details in section 4.3 and 4.4. It involves essentially two steps. Firstly, a reaction path modelling where the geochemistry of the aqueous solutions and minerals is simulated as a function of primary rock dissolution. Secondly, carbon isotope systematics was added to the model assuming equilibrium fractionation between various aqueous species and carbonate minerals formed. A model like this can then be compared with the measured CO_2 and $\delta^{13}C$ systematics, and various other parameters of importance like pH, and extent of reaction (ξ) to assess the possible source and reactions of carbon in the waters.

The results of the reaction path calculations are shown in Figures 9 and 10 as a function of extent of reaction (ξ). The calculations were performed at 25° and 100°C taken the initial rock to be basalt and the water to be meteoric in origin, saturated with atmospheric CO_2 (Fig. 9) and elevated CO_2 of unknown source of 5000 ppm (Fig. 10). The extent of reaction is then simply the moles of basalt dissolved per kg of solution. Upon basalt dissolution in waters saturated initially with atmospheric CO_2, the water pH is observed to have increased. This is caused by proton (H^+) consumption upon dissolution. As a result, the CO_2(aq) deprotonates to form HCO_3^- and CO_3^{2-} with increasing pH. The dissolution of the basalt also leaches rock forming elements into solution. As a consequence of both this behavior and the pH rise, secondary minerals are predicted to form; first simple hydroxides that are then followed by smectites, carbonates and zeolites at low temperatures and whereas at higher temperatures the hydroxides are absent. The dominant carbonate is calcite at all temperatures, but other carbonates like dolomite and ankerite may also exists in minor quantities (<10%). At elevated initial CO_2 concentrations, the aqueous speciation, pH, and mineral formation upon reaction progress is somewhat different. Due to the high CO_2 concentration the system pH becomes buffered at <7 due to ionization of CO_2 and basalt dissolution. Under these conditions, various types of carbonates may form particularly at low temperatures. When all the CO_2 has been mineralized, the pH of the solution rises rapidly to alkaline conditions. These observations are similar to those previously noted related to CO_2-water-basalt interaction (e.g. Stefánsson, 2010; Gysi and Stefánsson 2011).

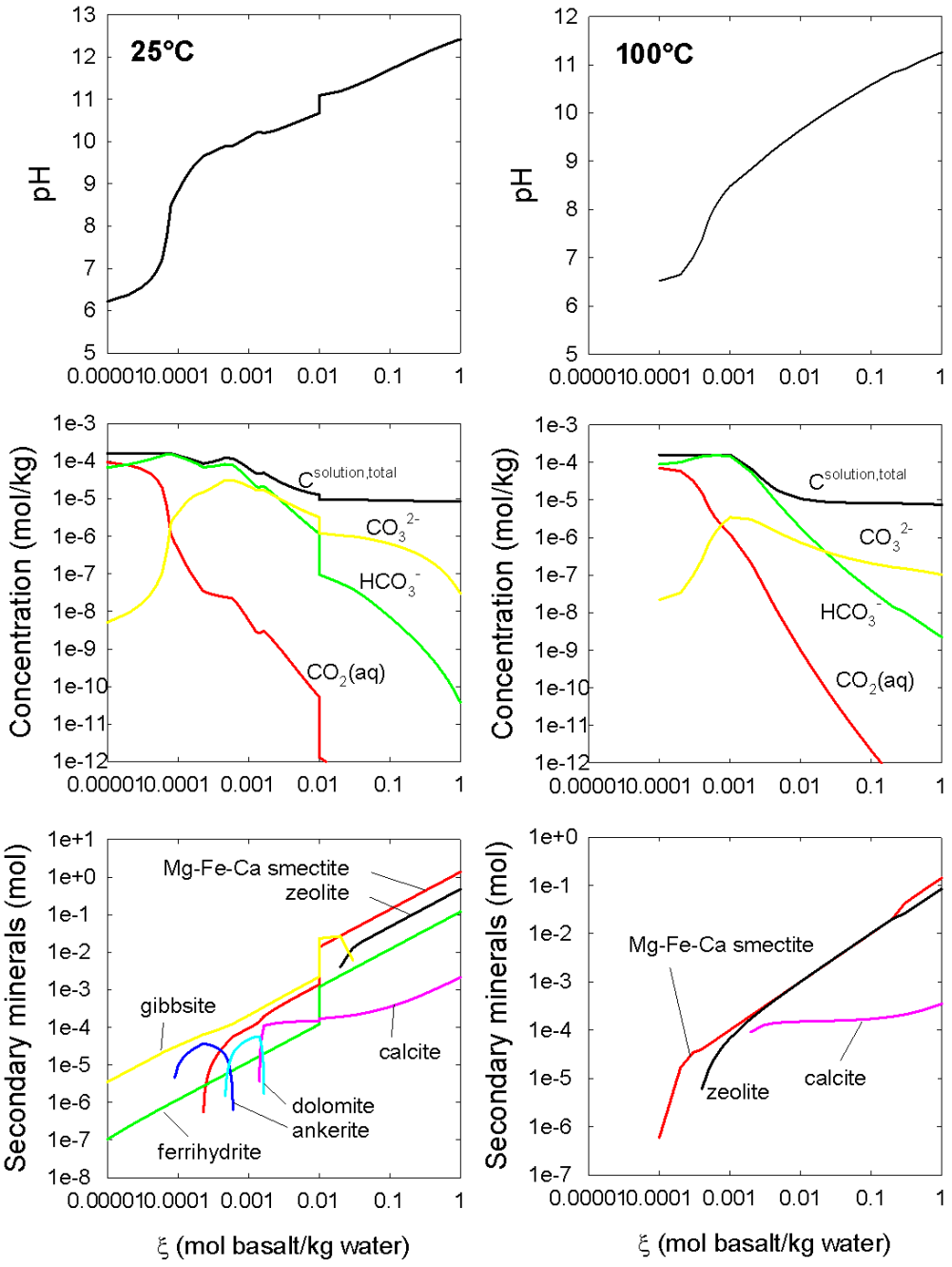

Figure 9 The results of the reaction path simulations for basalt dissolution into meteroic water initially saturated with atmospheric CO_2. Shown are the aqeuous carbon species distribution, pH, and secondary mineral formation as a function of reaction progress (ξ).

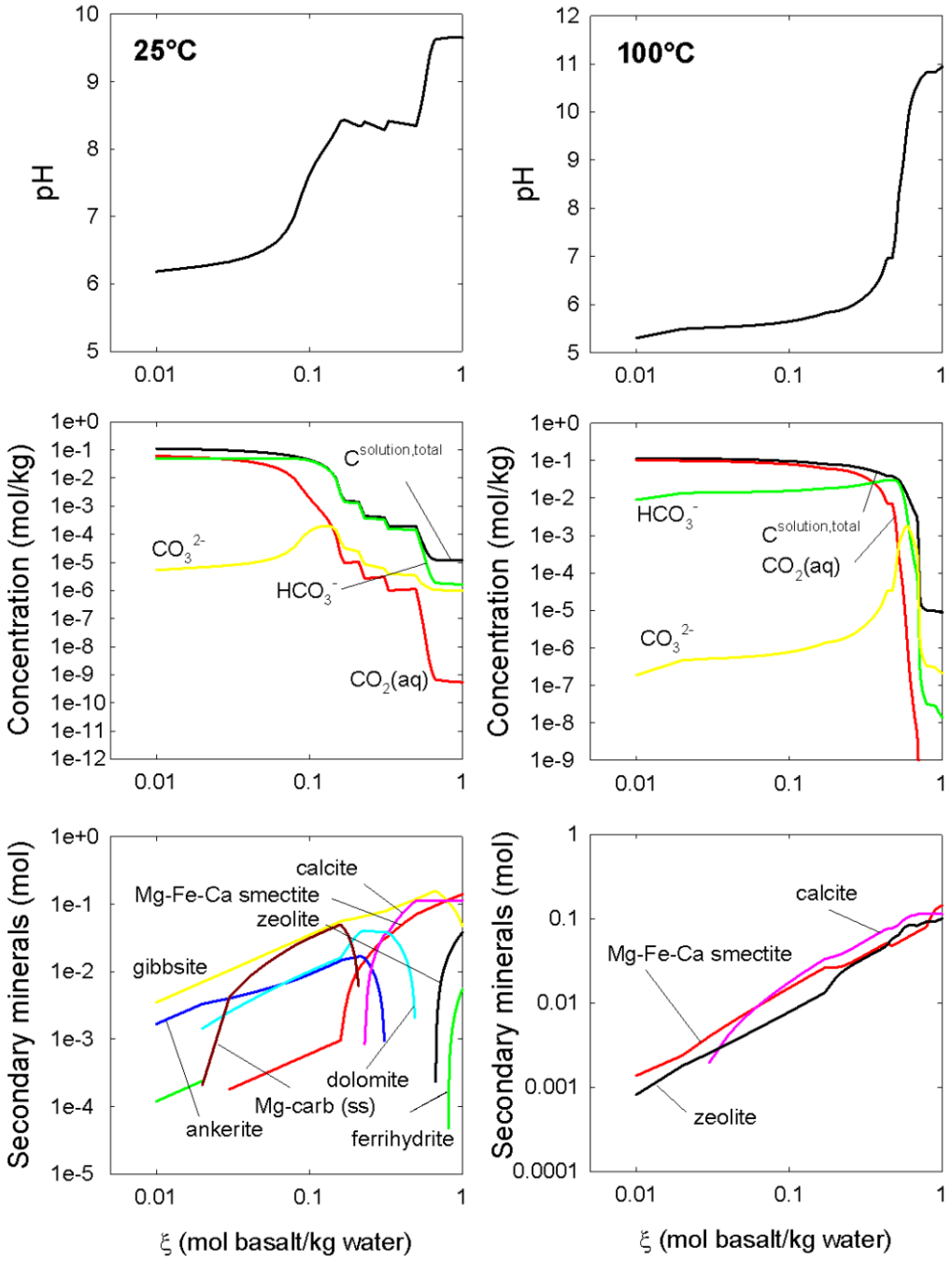

Figure 10 The results of the reaction path simulations for basalt dissolution into meteroic water initially containing 5000 ppm CO_2. Shown are the aqeuous carbon species distribution, pH, and secondary mineral formation as a function of reaction progress (ξ).

The result of the reaction path isotope modelling is shown in Figures 11 and 12 as a function of extent of reaction (ξ) and pH. The calculations were performed at 25 and 100°C taken the initial rock to be basalt and the water to be meteoric in origin, saturated with atmospheric CO_2 (Fig. 10) and elevated CO_2 of unknown source of 5000 ppm (Fig. 11). The $\delta^{13}C$ value of the starting solution saturated with atmospheric CO_2 was taken to be -

7‰ whereas the $\delta^{13}C$ value for the elevated CO_2 starting solution was chosen to be –3 ‰. The latter value is purely arbitrary but was chosen in order to explain the high and isotopically heavy CO_2 samples. The $\delta^{13}C$ values for the basalt was taken to be -7 ‰, close to the average for Icelandic basalts (Barry et al., 2014) and identical to the atmosphere for simplicity of the calculations.

Upon progressive water-rock interaction and at low initial CO_2 concentrations (atmospheric saturation), the pH of the solution changed from mildly acid to alkaline. The change in aqueous carbon speciation associated with the increase of pH resulted in $\delta^{13}C$ fractionation between various aqueous carbon species; the exact $\delta^{13}C$ values for $CO_2(aq)$, HCO_3^- and CO_3^{2-} tend to change as a function of reaction progress and pH. In addition to the changes in the carbonate speciation, calcite was predicted to form upon basalt dissolution further changing the $\delta^{13}C$ systematics. Initially, the total $\delta^{13}C$ value for the solution was similar to that of the starting water. However, $\delta^{13}C$ fractionation due to calcite formation resulted in a relative increase of the $\delta^{13}C$ values for calcite, as well as decrease of $\delta^{13}C$ values for aqueous species and the total solution. In addition, the relative distribution of carbonate species resulted in further decrease of the $\delta^{13}C$ solution value due to different fractionation factors between carbonate aqueous species and calcite. As a consequence, $\delta^{13}C$ values for aqueous solutions will decrease upon water-rock interaction with increasing pH within an isotopically closed system; such a decrease is solely related to fractionation upon aqueous speciation and calcite formation.

Similar trends were observed for $\delta^{13}C$ systematics for waters initially containing elevated CO_2 concentration and high isotope values (Fig. 12). Progressive water-rock interaction resulted in calcite formation being isotopically heavier than the total $\delta^{13}C$ value for the system. Nevertheless the aqueous CO_2 species are, isotopically lighter than calcite, and hence the total $\delta^{13}C$ value for the solution decreases. Due to the high initial CO_2 concentration, the system pH becomes buffered at <7 due to ionization of CO_2 and basalt dissolution. This results in somewhat constant $\delta^{13}C$ values for various components until CO_2 has been mineralized, which results in a pH increase, and a further decrease in the $\delta^{13}C$ solution values under alkaline conditions.

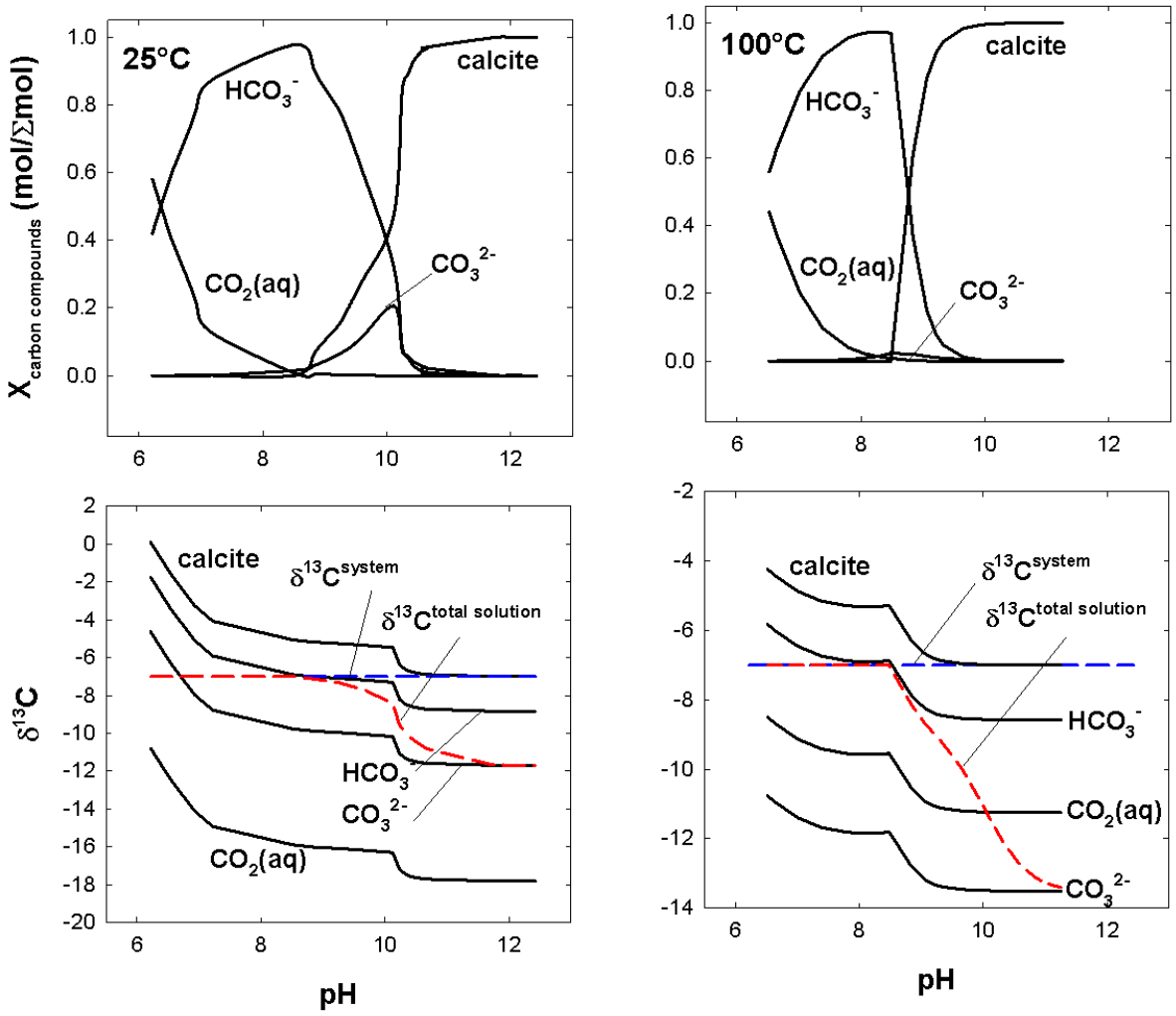

Figure 11 The results of the reaction path simulations for basalt dissolution into meteroic water initially saturated with atmospheric CO_2. The $\delta^{13}C$ value of the meteroic water and basalt was taken to be $\delta^{13}C$ -7‰. Shown are the aqeuous carbon species distribution, pH and secondary mineral formation as a function of reaction progress (ξ).

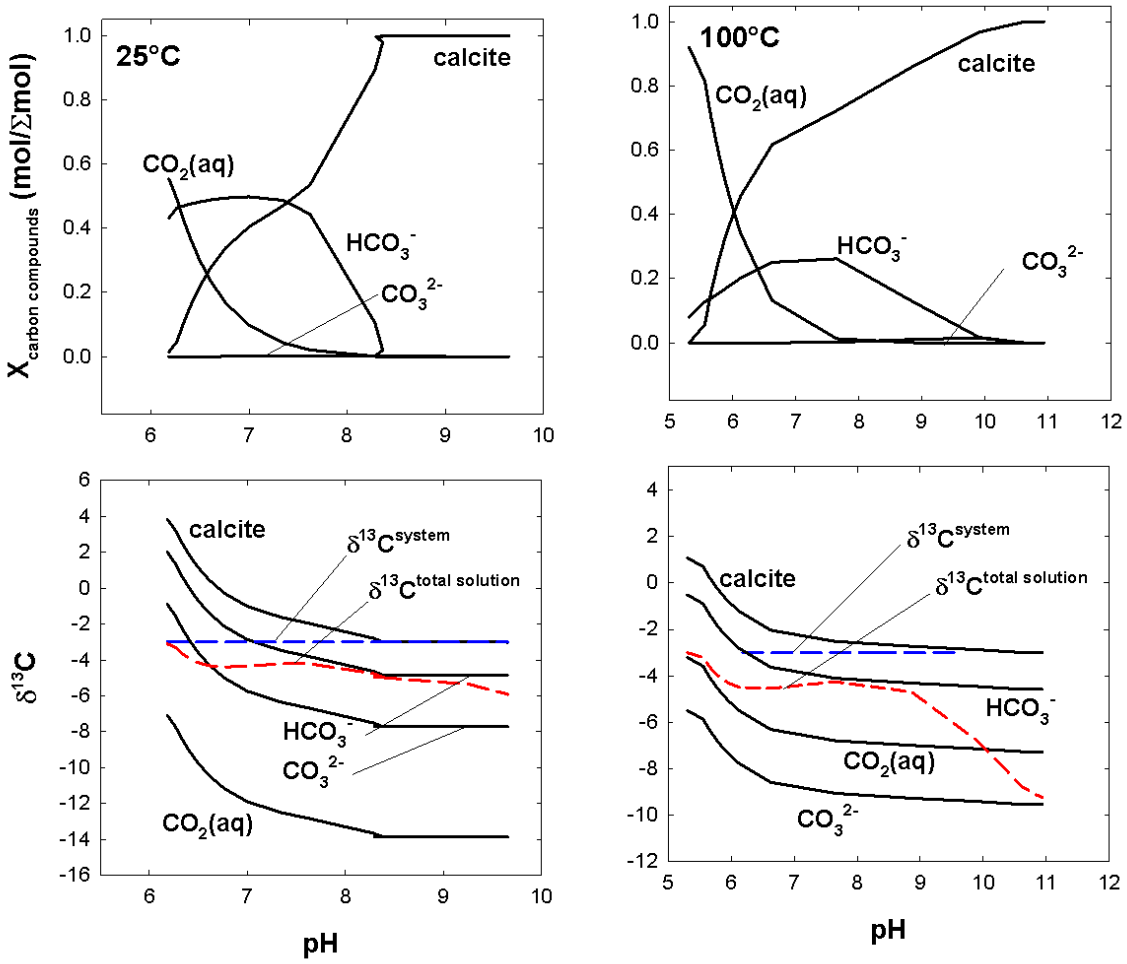

Figure 12 The results of the reaction path simulations for basalt dissolution into meteroic water initially containing 5000 ppm CO_2. The $\delta^{13}C$ value of the meteroic water was $\delta^{13}C$ -3‰ and basalt was taken to be $\delta^{13}C$ -7‰. Shown are the aqeuous carbon species distribution, pH, and secondary mineral formation as a function of reaction progress (ξ) and pH.

The results of the reaction path isotope modelling are compared with the measured $\delta^{13}C$ in low-temperature geothermal waters in Iceland in Figure 13. The observed decrease of $\delta^{13}C$ with increasing pH is clearly simulated, the cause being carbon isotope fractionation upon carbonic acid ionization and calcite formation. The CO_2 and $\delta^{13}C$ systematics of low-temperature waters that originate from meteoric water in equilibrium with atmospheric CO_2, and that react with the basalt should, be characterized by low CO_2 concentration (<50 ppm) and a variable $\delta^{13}C$ in the range of -5 to -15 ‰ (or even lower); the exact CO_2 concentration and $\delta^{13}C$ depend on the properties of the basalt and the pH of the water. The elevated CO_2 and isotopically heavy waters cannot be explained without the introduction of a high CO_2 source with $\delta^{13}C$ below -3‰. Assuming that the mantle has $\delta^{13}C$ -5 ‰ (Hoefs, 1997), a possible alternative CO_2 source needs to be introduced: a source which is presently unknown. Carbon fractionation upon calcite formation leads to high $\delta^{13}C$ values of calcite; this is both predicted in the model of this study and observed naturally (Hoefs, 1997). However, calcite dissolution cannot explain the elevated CO_2 and $\delta^{13}C$ values, as equilibrium between calcite and water under low-temperature conditions leads to relatively low CO_2 concentrations in the waters.

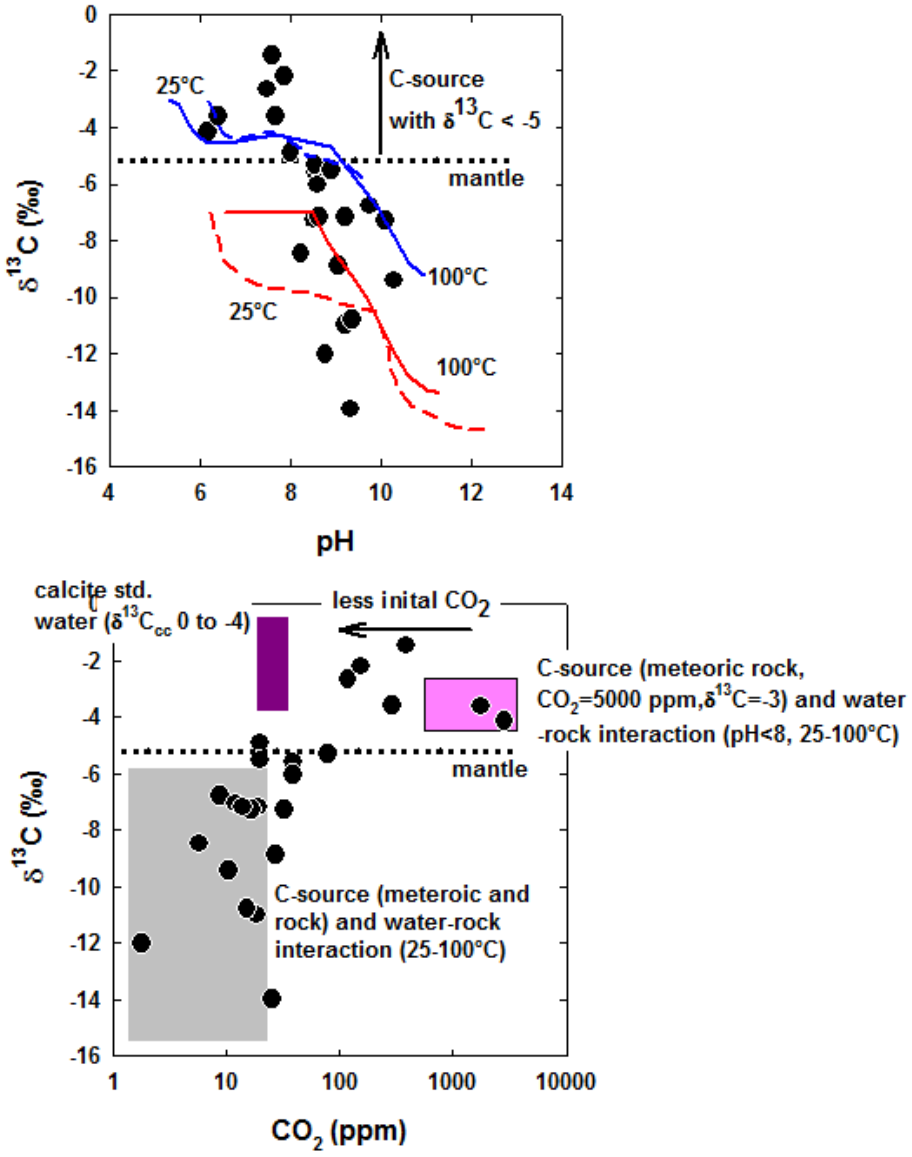

Figure 13 The comparison between the measured and simulated $\delta^{13}C$ and pH and $\delta^{13}C$ and CO_2 relationships. The blue and red curves represent the modelled trends for waters initally being CO_2 saturated and having 5000 ppm CO_2, respectively. The shaded areas show the simulated $\delta^{13}C$ and CO_2 relationship.

It is therefore concluded that progressive basalt dissolution, aqueous speciation and calcite formation play a major role in carbon isotope systematics of low-temperature geothermal waters in Iceland. For waters having low CO_2 concentrations (<50 ppm) and low $\delta^{13}C$ values (-5 to -15‰), the CO_2 source is thought to be derived from both atmospheric sources and from primary rocks; additionally the $\delta^{13}C$ systematics are controlled by the water-rock interaction. Waters that contain high CO_2 concentrations and high $\delta^{13}C$ values cannot be explained without the introduction of a highly concentrated CO_2 source having $\delta^{13}C$ value of less than -3‰. This source cannot be created by carbonate dissolution at shallow depth within the crust as this would result in relatively low CO_2 concentrations but high $\delta^{13}C$ value.

7 Conclusions

The carbon chemistry and stable carbon isotope systematics of low-temperature geothermal waters in Iceland was studied. The waters had temperatures ranging from 3° to 97°C, pH between 6.18 and 10.15 as well as dissolved inorganic carbon concentration from 1.8 to 2853 ppm. The carbon isotopes were found to be in the range $\delta^{13}C$ -1.46 to -13.96‰. The geochemistry of CO_2 and its sources and reactions in low-temperature geothermal water was approached in three ways; by carbonate mineral saturation, a component mixing model and by reaction path isotope modelling. Low-temperature geothermal waters were observed to be calcite saturated, suggesting that calcite may possibly form in low-temperature ground water systems. The source of the carbon in the water and the possible formation of calcite, along with the stable carbon isotope systematics cannot be explained simply by rock dissolution, atmospheric CO_2 input and organic matter decay. Instead, progressive basalt dissolution, aqueous speciation, and calcite formation play a major role in carbon isotope systematics and the carbon concentration of the low-temperature geothermal water. Upon progressive rock dissolution and increase in pH the aqueous speciation of the solution changes. The formation of calcite from different aqueous species results in $\delta^{13}C$ value changes in the calcite upon formation and results in $\delta^{13}C$ changes in the total solution. This is due to difference in fractionation factors between carbonate aqueous species and calcite. For waters that contain low CO_2 concentrations (<50 ppm) and low $\delta^{13}C$ values (-5 to -15‰) the CO_2 is thought to be derived from both atmospheric sources and primary rock dissolution. This is due to the variations of CO_2 concentrations and $\delta^{13}C$ values generated by the concentration of CO_2 and the exact $\delta^{13}C$ content of the basalt, and due to carbon isotope fractionation upon water-rock interaction. However, waters that contain high CO_2 concentrations and high $\delta^{13}C$ values cannot be explained without the introduction of a highly concentrated CO_2 source with a $\delta^{13}C$ value of less than -3‰. This source cannot be carbonate dissolution at shallow depth within the crust, as this would result in too low CO_2 concentrations although it could explain the $\delta^{13}C$ values of the waters. Mantle degassing through the crust is also unlikely as this would result in too low $\delta^{13}C$ values assuming the $\delta^{13}C$ value of the mantle to be -5 to -6%. Presently, an alternative CO_2 source of unknown origin has therefore been introduced as the cause of elevated CO_2 low-temperature geothermal waters in Iceland.

References

Arnórsson, S. (1970). Geochemical studies of thermal waters in the Southern Lowlands of Iceland. *Geothermics, 2* (1), 547-552.

Arnórsson, S., (1995a). Geothermal systems in Iceland: Structure and conceptual models-II. Low-temperature areas. *Geothermics, 24* (5), 603-629.

Arnórsson, S. (1995b). Geothermal systems in Iceland: Structure and conceptual models-I. High-temperature areas. *Geothermics, 24* (5), 561-602

Arnórsson, S. and Andrésdóttir, A., (1995). Processes controlling the distribution of boron and chlorine in natural waters in Iceland. *Geochimica et Cosmochimica Acta, 59* (20), 4125-4146.

Arnórsson, S. and Barnes, I. (1983). The nature of carbon dioxide waters in Snæfellsnes, western Iceland. *Geothermics, 12* (2), 171-176.

Arnórsson, S., Bjarnason, J.Ö., Giroud, N., Gunnarsson, I., Stefánsson, A. (2006). Sampling and analysis of geothermal fluids. *Geofluids, 6,* 203-216.

Arnórsson, S., and Gíslason, S.R. (1990). Um uppruna lághitasvæða á Íslandi. *Náttúrufræðingurinn, 60* (1), 39-56.

Arnórsson, S. and Ólafsson, G., (1986). A Model for the Reykholtsdalur and the Upper-Árnessýsla Geothermal Systems with a Discussion on some Geological and Geothermal Processes in SW-Iceland. *Jökull, 36,*1-9

Arnórsson, S. and Sveinbjörnsdóttir, Á,E. (2000). Age and chemical evolution of groundwaters in Skagafjörður, Iceland. *Journal of Geochemical Exploration, 69-70,* 459-463.

Axelsson, G., Gunnlaugsson, E., Jónsson, T., Ólafsson, M., (2010). Low-temperature geothermal utilization in Iceland-Decades of experience. *Geothermics, 39,* 329-338.

Barry, P.H., Hilton, D.R., Füri, E., Halldórsson, S.A., Grönvold, K., (2014). Carbon isotope abundance systematics of Icelandic geothermal gases, fluids and subglacial basalts with implications for mantle plume- related CO_2 fluxes. *Geochimica et Cosmochimica Acta, 134,* 74-99.

Björnsson, A., Axelsson, G., Flóvenz, Ó.G. (1990). Uppruni hvera og lauga á Íslandi. *Náttúrufræðingurinn, 60* (1), 15-38.

Bottinga, Y. (1969). Calculated fractionation factors for carbon and hydrogen isotope exchange in the system calcite-carbon dioxide-graphite-methane-hydrogen-water vapor. *Geochimica et Cosmochimica Acta, 33,* 49-64.

Browne, P.R.L, (1978). Hydrothermal alteration in active geothermal fields. Annual review, *Earth and Planetary Science Letters,* 6, 229-250.

Böðvarsson, G. (1961). Physical Characteristics of Natura Heat Resources in Iceland. *Jökull, 11,* 29-38.

Coplan. T.B. (1994). Reporting of stable hydrogen, carbon and oxygen isotopic abundances. *Pure and applied chemistry, 66* (2), 273-276.

Deer,W.A., Howie, R.A., Zussman, J.(1992). *An introduction to The Rock Forming Minerals (2nd ed*). London: Pearson Education Limited.

Deuser, W.G. and Degens. E.T. (1967). Carbon isotope fractionation in the system CO_2(gas)-CO_2(aqueous)-HCO_3^-(aqueous). *Nature, 215* (5105), 1033-1035.

Einarsson, P. (1991). Earthquakes and present-day tectonism in Iceland. *Tectonophysics, 189,* 261-279.

Emrich, K., Ehhalt, D.H., Vogel, J.C. (1970). Carbon isotope fractionation during the precipitation of calcium carbonate. *Earth and Planetary Science Letters, 8*, 363-371.

Gíslason, S.R., (2012). *Kolefnis hringrásin.* Reykjavík: Hið íslenska bókmenntafélag.

Georgsson, L.S., Jóhannesson, H., Gunnlaugsson, E., Haraldsson, G.I (1984). Geothermal Exploration of the Reykholt Thermal System in Borgarfjörður, West Iceland. *Jökull, 34* , 105-116.

Gysi, A.P., and Stefánsson, A. (2011). CO_2-water-basalt interaction. Numerical simulation of low temperature CO_2 sequestration into basalts. *Geochimica et Cosmochima Acta, 75*, 4728-4751.

Gysi, A. P., and Stefánsson, A., (2012).CO_2-water-basalt interaction. Low temperature experiments and implications for CO_2 sequestration into basalts. *Geochimica et Cosmochimica Acta, 81*, 129-152.

Halas, S., Szaran, J., Niezgoda, H. (1997). Experimental determination of carbon isotope equilibrium fractionation between dissolved carbonate and carbon dioxide. *Geochimica et Cosmochimica Acta, 61* (13), 2691-2695.

Hoefs, J. (1997). *Stable Isotope Geochemistry (4th ed.).* Germany:Springer-Verlag.

Jóhannesson, H. (1980). Jarðalagaskipan og þróun rekbelta á Vesturlandi. *Náttúrufræðingurinn, 50* (1), 13-31.

Jóhannesson, H. (1982). *Yfirlit um Jarðfræði Snæfellsnes*, in Árbók Ferðafélag Íslands 1982, 151-172.

Malinin, S.D., Kropotova, O.I., Grinenko, V.A. (1967). Experimental determination of equilibrium constants for carbon isotope exchange in the system CO_2(g)- HCO_3-(sol.) under hydrothermal conditions, *Geokhimiya, 8*, 927-935.

Marshall, J. D., Brooks, J.R & Lajtha, K. (2007). Sources of variations in stable isotopes in plants (2^{nd} ed). In Michener, R. & Lajtha, K. (editors*), Stable isotopes in ecology and environmental science- ecological methods and concepts* (22-50). Oxford: Blackwell Publishing.

Mehegan, J.M., P.T. Robinson and J.R. Delaney. (1982). Secondary mineralization and geothermal alteration in the Reydarfjordur drill core, east Iceland. *Journal of Geophysical Research, 87*, 6511-6524.

McNichol, A.P., Jones, G.A., Hutton, D.L., Gagnon, A.R. (1994). The rapid preparation of seawater CO_2 for radiocarbon analysis at the national ocean sciences AMS facility. *Radiocarbon, 36*, 237-246.

Mook, W.G., Bommerson, J.C., Staverman, W.H. (1974). Carbon isotope fractionation between dissolved bicarbonate and gaseous carbon dioxide. *Earth and Planetary Science Letters, 22*, 169-176.

Myrttinen, A., Becker,V., Mayer, B., Barth, J.A.C. (2014). Stable caron isotope fractionation data between H_2CO_3 and CO_2(g) extended to 120°C. *Rapid Communications in Mass Spectrometry, 28* (15), 1691-1696

Neuhoff, P.S., Fridriksson, Th., Arnórsson, S., Bird, T.K. (1999). Porosity evolution and mineral paragenesis during low-grade metamorphism of basaltic lavas at Teigarhorn eastern Iceland. *American Journal of Science, 299*, 467-501

Ólafsson M., Hauksdóttir S., Thórhallsson S. and Snorrason Th. (2005). Calcite Scaling at Selfossveitur Hitaveita, S-Iceland, when Mixing Waters of Different Chemical Composition. *Proceedings to the World Geothermal Congress 24-29 April 2005*. Antalya, Turkey: World geothermal Congress 2005.

Parkhurst, D.L. and Appelo, C.A.J., (1999). *User's guide to PHREEQC (Version 2)--a computer program for speciation, batch-reaction, one-dimensional transport, and inverse geochemical calculations*. Report 99-4259, U.S. Geological Survey, Water-Resources Investigations.

Romanek, C.S., Grossman, E.L., Morse, J.W. (1992). Carbon isotope fractionation in synthetic aragonite and calcite: Effects of temperature and precipitation rate. *Geochimica et Cosmochimica Acta, 56*, 419-430.

Rubinson, M. and Clayton, R.N., (1969). Carbon-13 fractionation between aragonite and calcite. *Geochimica et Cosmochimica Acta, 33*, 997-1002.

Sharp, Z. (2007). *Principles of stable isotope geochemistry*. New Jersey: Pearson-Prentice Hall.

Stefánsson, A. (2010). Low-temperature alteration of basalts – the effects of temperature, acids and time on mineralization and water chemistry. *Jökull, 60*, 165-184.

Sveinbjörnsdóttir, Á., Heinemeier, J., Arnórsson, S. (1995). Origin of ^{14}C in Icelandic groundwater. *Radiocarbon, 37* (2), 551-565.

Szaran, J. (1997). Achievement of carbon isotope equilibrium in the system HCO_3-(solution)-CO_2 (gas). *Chemical Geology, 142*, 79-86.

Torfason, H. (2003) *Jarðhitakort af Íslandi og gagnasafn um jarðhita*. Reykjavík: Orkustofnun. OS-2003/062

Vogel, J.C., Grootes, P.N., Mook, W.G. (1970). Isotopic fractionation between gaseous and dissolved carbon dioxide. *Z. Physik, 230*, 225-238.

Zhang, J., Quay, P.D., Wilbur, D.O. (1995). Carbon isotope fractionation during gas-water exchange and dissolution of CO_2. *Geochimica et Cosmochimica Acta, 59* (4), 107-114.